Global parameterization and validation of a two-leaf light use efficiency model for predicting gross primary production across FLUXNET sites

Yanlian Zhou, Xiaocui Wu, Weimin Ju, Jing M. Chen, Shaoqiang Wang, Huimin Wang, Wenping Yuan, T. Andrew Black, Rachhpal Jassal, Andreas Ibrom, et al.

AGU PUBLICATIONS

JGR

Journal of Geophysical Research: Biogeosciences

RESEARCH ARTICLE
10.1002/2014JG002876

Key Points:
- TL-LUE performed in general better than commonly used MOD17 algorithm
- Tight relationships between LUE of sunlit and shaded leaves with LUE of MOD17
- Lower sensitivity of TL-LUE to PAR input data than that of MOD17

Correspondence to:
W. Ju,
juweimin@nju.edu.cn

Citation:
Zhou, Y., et al. (2016), Global parameterization and validation of a two-leaf light use efficiency model for predicting gross primary production across FLUXNET sites, *J. Geophys. Res. Biogeosci.*, *121*, 1045–1072, doi:10.1002/2014JG002876.

Received 9 DEC 2014
Accepted 2 DEC 2015
Accepted article online 7 DEC 2015
Published online 6 APR 2016

Global parameterization and validation of a two-leaf light use efficiency model for predicting gross primary production across FLUXNET sites

Yanlian Zhou[1,2], Xiaocui Wu[3,2], Weimin Ju[3,4], Jing M. Chen[3,2], Shaoqiang Wang[5], Huimin Wang[5], Wenping Yuan[6], T. Andrew Black[7], Rachhpal Jassal[7], Andreas Ibrom[8], Shijie Han[9], Junhua Yan[10], Hank Margolis[11], Olivier Roupsard[12,13], Yingnian Li[14], Fenghua Zhao[5], Gerard Kiely[15], Gregory Starr[16], Marian Pavelka[17], Leonardo Montagnani[18,19], Georg Wohlfahrt[20,21], Petra D'Odorico[22], David Cook[23], M. Altaf Arain[24], Damien Bonal[25], Jason Beringer[26], Peter D. Blanken[27], Benjamin Loubet[28], Monique Y. Leclerc[29], Giorgio Matteucci[30], Zoltan Nagy[31], Janusz Olejnik[32,33], Kyaw Tha Paw U[34,35], and Andrej Varlagin[36]

[1]Jiangsu Provincial Key Laboratory of Geographic Information Science and Technology, School of Geographic and Oceanographic Sciences, Nanjing University, Nanjing, China, [2]Joint Center for Global Change Studies, Beijing, China, [3]International Institute for Earth System Sciences, Nanjing University, Nanjing, China, [4]Jiangsu Center for Collaborative Innovation in Geographic Information Resource Development and Application, Nanjing, China, [5]Key Laboratory of Ecosystem Network Observation and Modeling, Institute of Geographic Sciences and Natural Resources Research, Chinese Academy of Science, Beijing, China, [6]State Key Laboratory of Earth Surface Processes and Resource Ecology, Future Earth Research Institute, Beijing Normal University, Beijing, China, [7]Faculty of Land and Food Systems, University of British Columbia, Vancouver, British Columbia, Canada, [8]Department of Environmental Engineering, Technical University of Denmark (DTU), Kgs. Lyngby, Denmark, [9]Institute of Applied Ecology, Chinese Academy of Sciences, Shenyang, China, [10]South China Botanical Garden, Chinese Academy of Sciences, Guangzhou, China, [11]Centre for Forest Studies, Faculty of Forestry, Geography and Geomatics, Laval University, Quebec City, Quebec, Canada, [12]CIRAD-Persyst, UMR Ecologie Fonctionnelle and Biogéochimie des Sols et Agroécosystèmes, SupAgro-CIRAD-INRA-IRD, Montpellier, France, [13]CATIE (Tropical Agricultural Centre for Research and Higher Education), Turrialba, Costa Rica, [14]Northwest Institute of Plateau Biology, Chinese Academy of Sciences, Xining, China, [15]Environmental Research Institute, Civil and Environmental Engineering Department, University College Cork, Cork, Ireland, [16]Department of Biological Sciences, University of Alabama, Tuscaloosa, Alabama, USA, [17]Laboratory of Plants Ecological Physiology, Institute of Systems Biology and Ecology AS CR, Prague, Czech Republic, [18]Forest Services, Autonomous Province of Bolzano, Bolzano, Italy, [19]Faculty of Sciences and Technology, Free University of Bolzano, Bolzano, Italy, [20]Institute for Ecology, University of Innsbruck, Innsbruck, Austria, [21]European Academy of Bolzano, Bolzano, Italy, [22]Grassland Sciences Group, Institute of Agricultural Sciences, ETH Zurich, Switzerland, [23]Atmospheric and Climate Research Program, Environmental Science Division, Argonne National Laboratory, Argonne, Illinois, USA, [24]McMaster Centre for Climate Change and School of Geography and Earth Sciences, McMaster University, Hamilton, Ontario, Canada, [25]INRA Nancy, UMR EEF, Champenoux, France, [26]School of Earth and Environment, The University of Western Australia, Crawley, Australia, [27]Department of Geography, University of Colorado Boulder, Boulder, Colorado, USA, [28]UMR ECOSYS, INRA, AgroParisTech, Université Paris-Saclay, Thiverval-Grignon, France, [29]Department of Crop and Soil Sciences, College of Agricultural and Environmental Sciences, University of Georgia, Athens, Georgia, USA, [30]Viea San Camillo Ed LellisViterbo, University of Tuscia, Viterbo, Italy, [31]MTA-SZIE Plant Ecology Research Group, Szent Istvan University, Godollo, Hungary, [32]Meteorology Department, Poznan University of Life Sciences, Poznan, Poland, [33]Department of Matter and Energy Fluxes, Global Change Research Center, Brno, Czech Republic, [34]Department of Land, Air and Water Resources, University of California, Davis, California, USA, [35]Joint Program on the Science and Policy of Global Change, Massachusetts Institute of Technology, Cambridge, USA, [36]A.N. Severtsov Institute of Ecology and Evolution, Russian Academy of Sciences, Moscow, Russia

Abstract Light use efficiency (LUE) models are widely used to simulate gross primary production (GPP). However, the treatment of the plant canopy as a big leaf by these models can introduce large uncertainties in simulated GPP. Recently, a two-leaf light use efficiency (TL-LUE) model was developed to simulate GPP separately for sunlit and shaded leaves and has been shown to outperform the big-leaf MOD17 model at six FLUX sites in China. In this study we investigated the performance of the TL-LUE model for a wider range of biomes. For this we optimized the parameters and tested the TL-LUE model using data from 98 FLUXNET sites which are distributed across the globe. The results showed that the TL-LUE model performed in general better than the MOD17 model in simulating 8 day GPP. Optimized maximum light use efficiency of shaded leaves (ε_{msh}) was 2.63 to 4.59 times that of sunlit leaves (ε_{msu}). Generally, the relationships of ε_{msh} and ε_{msu} with ε_{max}

were well described by linear equations, indicating the existence of general patterns across biomes. GPP simulated by the TL-LUE model was much less sensitive to biases in the photosynthetically active radiation (PAR) input than the MOD17 model. The results of this study suggest that the proposed TL-LUE model has the potential for simulating regional and global GPP of terrestrial ecosystems, and it is more robust with regard to usual biases in input data than existing approaches which neglect the bimodal within-canopy distribution of PAR.

1. Introduction

Gross primary productivity (GPP) is a key component of the terrestrial carbon cycle and a principal indicator for biosphere carbon fluxes [*Zhang et al*., 2009; *Yuan et al*., 2010]. The reliable estimation of GPP is a prerequisite for accurately determining carbon sequestration rates by terrestrial ecosystems [*Sakamoto et al*., 2011]. GPP at the ecosystem level can be estimated with good accuracy from measurements of CO_2 fluxes at eddy covariance towers [*Baldocchi*, 2003]. At regional and global scales, GPP can be calculated by a number of ecosystem models [*Foley et al*., 1996; *Liu et al*., 1997; *Beer et al*., 2010; *Ryu et al*., 2011]. The application of process-based ecosystem models is constrained by the requirements of many model drivers and parameters. In contrast, light use efficiency (LUE) models, which calculate GPP as the product of absorbed photosynthetically active radiation (APAR) and LUE, require fewer inputs and are computationally less demanding and easy to parameterize [*Prince and Goward*, 1995; *Running et al*., 2004; *Yuan et al*., 2007]. Therefore, these models have been more and more widely used to calculate regional and global GPP. For example, through combining remotely sensed leaf area index (LAI) and distributed climate data, the MOD17 model is able to produce the global GPP product (MOD17A2) in near real time.

Most widely used LUE models, such as Carnegie-Ames-Stanford approach [*Potter et al*., 1993], the MOD17 algorithm [*Running et al*., 2004], Vegetation Photosynthesis Model [*Xiao et al*., 2004], eddy covariance (EC)-LUE [*Yuan et al*., 2007], and Greenness and Radiation models [*Gitelson et al*., 2006; *Wu et al*., 2011], treat the vegetation canopy as a big leaf with a simple mathematical form assuming that GPP linearly increases with incoming photosynthetically active radiation (PAR). However, in fact, GPP is not always linearly increasing with incoming PAR. Different groups of leaves (sunlit and shaded) within the plant canopy have different levels of exposure to direct sunlight and consequently different LUE values [*De Pury and Farquhar*, 1997; *Wang and Leuning*, 1998; *Chen et al*., 1999; *Friend*, 2001]. Sunlit leaves (which simultaneously absorb both direct and diffuse radiation) are easily light saturated, leading to low LUE (ε_{msu}) values [*Gu et al*., 2002]. In contrast, photosynthesis of shaded leaves (which only absorb diffuse radiation) is normally limited by low radiation and increases linearly with increasing absorbed PAR. As a consequence, the LUE of shaded leaves (ε_{msh}) is relatively high [*De Pury and Farquhar*, 1997; *Wang and Leuning*, 1998; *Chen et al*., 1999; *Friend*, 2001]. However, the currently most widely used LUE models do not explicitly account for the difference in APAR and LUE of sunlit and shaded leaves within the canopy, which has been recently shown to result in biased values of estimated GPP [*Zhang et al*., 2011; *Propastin et al*., 2012; *He et al*., 2013].

One, so far, unconsidered reason that leads to variation in LUE is that diffuse and direct radiation affect canopy LUE in different ways. LUE is shown to increase with the diffuse fraction through model simulations [*Sinclair and Shiraiwa*, 1993; *de Pury and Farquhar*, 1997; *Cohan et al*., 2002; *Ibrom et al*., 2006] and observations [*Rochette et al*., 1996; *Roderick et al*., 2001; *Choudhury*, 2001; *Gu et al*., 2002; *Alton et al*., 2007; *Alton*, 2008]. Therefore, an increase in diffuse radiation results in increase of carbon uptake [e.g., *Gu et al*., 2003; *Cai et al*., 2009]. For example, *Hollinger et al*. [1994] found that carbon uptake in a New Zealand beach forest increased by 50% on cloudy days relative to the value on clear days. *Gu et al*. [2003] detected a 20% increase in forest photosynthesis after the Pinatubo Volcano eruption in 1991, which increased diffuse radiation through scattering by atmospheric particles. Similar increases of LUE under diffuse sunlight were also reported in other studies [e.g., *Niyogi et al*., 2004; *Urban et al*., 2007; *Zhang et al*., 2011]. So a modification of the traditional LUE approach which considers the variation of LUE at the canopy scale by allowing for the variation of LUE under different conditions of radiation was suggested [*Ibrom et al*., 2008].

To overcome the weakness of LUE models, *He et al*. [2013] developed a two-leaf LUE model (TL-LUE) that stemmed from the MOD17 model [e.g., *Running et al*., 2004; *Turner et al*., 2006] and the approach of the process-based boreal ecosystem productivity simulator (BEPS) [*Chen et al*., 1999] and tested it against GPP measured at six ChinaFLUX sites. The TL-LUE model considers the difference in LUE and absorbed radiation

of sunlit and shaded leaves. The composition and function of ecosystems vary greatly across different locations on the globe, and thus, the TL-LUE model needs to be tested and validated at other biomes. Moreover, the LUE of sunlit and shaded leaves varies with ecosystem types [*Rochette et al*., 1996; *Lamaud et al*., 1997; *Gu et al*., 2002; *He et al*., 2013]. However, the values of ε_{msu} and ε_{msh} and their variation among different ecosystems are not known. Therefore, ε_{msu} and ε_{msh} in the TL-LUE model need to be calibrated rigorously for accurate estimation of GPP. Globally, the network of eddy covariance (EC) towers (FLUXNET) now covers a wide range of ecosystems across different climate zones [*Falge et al*., 2002; *Law et al*., 2002; *Baldocchi*, 2014]. EC-derived GPP (GPP_EC) values provide a unique opportunity for validating models and calibrating or optimizing model parameters [*Running et al*., 1999; *King et al*., 2011; *Baldocchi*, 2014].

The TL-LUE model is driven by meteorological data (vapor pressure deficit (VPD), PAR, and air temperature (T_a)) and remotely sensed data (*f*PAR or LAI). When it is used for simulating GPP over large areas, the errors of simulated GPP are partially caused by uncertainties in the input data, which are the same as those of the most widely used LUE models, such as the Moderate Resolution Imaging Spectroradiometer (MODIS) GPP algorithm [*Zhao et al*., 2005; *Leuning et al*., 2005]. VPD and T_a have the same impacts on the MOD17 and TL-LUE models, while PAR and LAI (or *f*PAR) have different impacts, due to the differing representations of within-canopy radiative transfer. Moreover, incoming shortwave radiation or PAR from regularly gridded reanalysis data sets (such as reanalysis data provided by European Centre for Medium-Range Weather Forecasts and National Centers for Environmental Prediction/National Center for Atmospheric Research (NCEP/NCAR)) and remotely sensed LAI data sets might have systematic errors >20% [*Zhao and Running*, 2006; *Fang et al*., 2012; *Jia et al*., 2013]. Thus, there is need to assess the sensitivity of TL-LUE and MOD17 models to PAR and LAI in estimating GPP.

The overarching objective of this study is to examine the robustness of the TL-LUE model using GPP derived from eddy covariance CO_2 flux measurements at 98 globally distributed flux towers. Specific objectives are to (1) evaluate the performance of the TL-LUE model for simulating GPP in different ecosystem types, (2) determine the maximum light use efficiency of sunlit and shaded leaves for different ecosystems, and (3) analyze the sensitivity of the TL-LUE model to uncertainties in the PAR and LAI input data.

2. Data and Methods

2.1. Data Used

2.1.1. Global Land Cover (30 m) (GlobeLand30) Data Set

In order to constrain the influences of land cover heterogeneity around towers GPP on model calibration and validation, the GlobeLand30 data sets in 2000 and 2010 with a spatial resolution of 30 m were used for selecting towers with relatively homogenous land cover. These data sets were produced by the National Geomatics Center of China. They both cover land area from 80°N to 80°S and include 10 land cover types, namely, cultivated land (crop), forest, grassland, shrubland, wetland, water bodies, tundra, artificial surfaces, bareland, permanent snow, and ice. These data sets were donated to the United Nations with the aim of contributing to research on sustainable development and climate change [*Jun et al*., 2014] and have been widely used in many studies [*Cao et al*., 2014; *Chen et al*., 2015; *Manakos et al*., 2014; *Brovelli et al*., 2015]. More detailed information on these data sets was described on the website of http://glc30.tianditu.com.

2.1.2. Eddy Covariance and Meteorological Data

Eddy covariance data from the LaThuile FLUXNET database were used to parameterize and validate the TL-LUE model. Sites were first selected on the basis of data availability of daily GPP, VPD, T_a, and PAR. Sites with missing data of more than 20% during the growing seasons were excluded from this analysis. Then, the GlobeLand30 in 2000 and 2010 was employed in conjunction with Google maps to exclude some flux sites with very heterogeneous vegetation types to minimize the impact of land cover heterogeneity on optimized model parameters. The sites were selected in following steps. For each flux site, we extracted the area proportions of 10 different land cover types over the central 1 km × 1 km (for crop, grass, savannas, open shrub, and woody savannas) or 3 km × 3 km (for forests) area around the tower in years of 2000 and 2010 and then averaged the area proportions in the 2 years. For sites of forests indicated by the site description in the LaThuile FLUXNET database, shrubland was merged into forest in calculating the area proportions of forests based on the GlobeLand30 and Google maps, as forest was often misclassified as shrubland using remote sensing data. There are a few sites labeled as grass in the site description. The calculated area proportion of grassland was less than 0.1, while the proportion of cultivated land was above 0.8. For these sites, cultivated land was

Table 1. Model Parameters Used for Different Vegetation Types

Vegetation Type[a]	DBF	ENF	EBF	MF	Grass	Crop	Savannas	OS	WS
ε_{max}(g CMJ^{-1})[b]	1.04	1.01	1.26	1.12	0.60	0.60	0.89	0.77	0.77
T_{amin_max} (°C)	7.94	8.31	9.09	8.5	12.02	12.02	8.61	8.8	11.39
T_{amin_min} (°C)	−8	−8	−8	−8	−8	−8	−8	−8	−8
VPD_{max} (kpa)	4.1	4.1	4.1	4.1	4.1	4.1	4.1	4.1	4.1
VPD_{min} (kpa)	0.93	0.93	0.93	0.93	0.93	0.93	9.3	9.3	9.3
Clumping index (Ω^c)	0.8	0.6	0.8	0.7	0.9	0.9	0.8	0.8	0.8

[a]DBF: deciduous broadleaf forest; ENF: evergreen needleleaf forest; EBF: evergreen broadleaf forest; MF: mixed forest; Grass: grass; Crop: crop; Savannas: savannas; OS: open shrub; WS: woody savannas.
[b]*Running et al.* [2000]. The values were default values used in the MOD17 model for calculating MODIS GPP product. T_{amin_max}, T_{amin_min}, VPD_{max}, and VPD_{min}were used in both the MOD17 algorithm and TL-LUE model.
[c]*Tang et al.* [2007] Clumping index (Ω) was only used in the TL-LUE model.

merged into grass land in calculating area proportion of grassland based on the GlobeLand30 and Google maps. The flux sites were selected according to two conditions: the area proportion of the dominant cover type is larger than a threshold and the dominant cover type is the same as that extracted from the LaThuile FLUXNET database. In order to balance the number of flux sites and their land cover homogeneity, the area proportion threshold of the dominant cover type was set as 0.5. As there were limited deciduous broadleaf forests (DBF) and mixed forests (MF) sites, five sites with area proportions of dominant cover types less than 0.5 were kept, including two DBF sites (FR-Fon and FR-Hes with area proportions of dominant cover types equal to 0.45 and 0.37, respectively) and three MF sites (BE-Bra, CA-TP4, and DE-Har with area proportions of dominant cover types equal to 0.34, 0.47, and 0.31, respectively). Open shrub (OS), savannas (S), and woody savannas (WS) were not differentiated in the GlobeLand30 data sets. In calculating the area proportions of OS, S, and WS sites, shrubland was accordingly treated as OS, S, and WS following the cover types extracted from the LaThuile FLUXNET database, and the highest area proportion among 10 types was considered as the proportion of OS, S, and WS. The area proportions of different cover types for each site were shown in Table A1 in Appendix A.

In total, measurements of 268 site years from 98 sites were used in this study, including 32 evergreen needleleaf forests (ENF), 6 evergreen broadleaf forests (EBF), 10 deciduous broadleaf forests (DBF), 16 mixed forests (MF), 14 crop (Crop), 12 grass (Grass), 2 savannas (S), 4 open shrub (OS), and 2 woody savannas (WS) sites. Out of these 98 flux sites, 78 sites (79.6%) have area proportions of dominant vegetation types higher than 0.7, in which 60 sites (61.2%) have area proportions of dominant vegetation types above 0.8. These sites are distributed over East Asia, United States, Canada, and Europe. Detailed information on these sites is given in Table A2 in Appendix A. Measured GPP values from 195 randomly selected site years representing different vegetation types (VTs) were used to estimate the optimal parameter (maximum light use efficiencies) values, and the remaining 73 site years of measurements were used for model validation.

All flux data were processed in a consistent manner within the FLUXNET project [*Baldocchi et al.*, 2001; *Baldocchi*, 2008] as described by *Papale and Valentini* [2003], *Reichstein et al.* [2005], and *Papale et al.* [2006]. GPP data were derived from the net ecosystem CO_2 exchange (NEE) measured using the eddy covariance

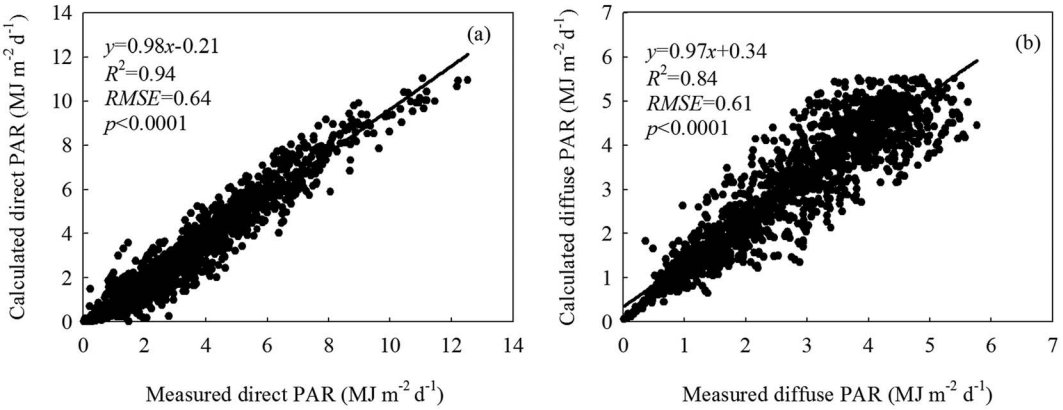

Figure 1. Comparison between measured and modeled (a) direct PAR and (b) diffuse PAR.

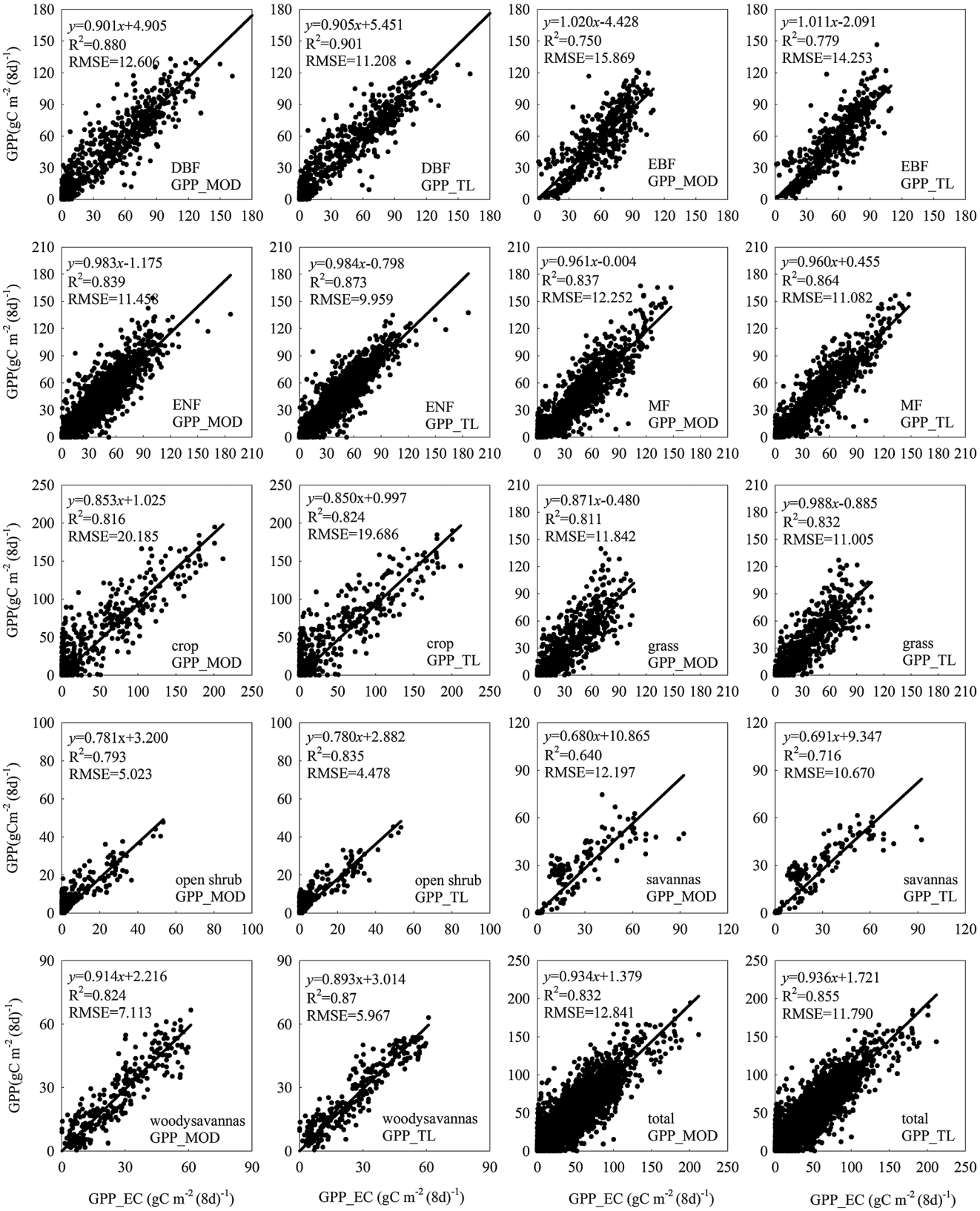

Figure 2. Comparison of 8 day GPP calculated using the MOD17 (GPP_MOD) and TL-LUE (GPP_TL) models with corresponding tower measurements (GPP_EC) for the site years used in the optimization. Both the MOD17 and TL-LUE models were driven using optimized parameters, smoothed LAI, and tower-based meteorological data.

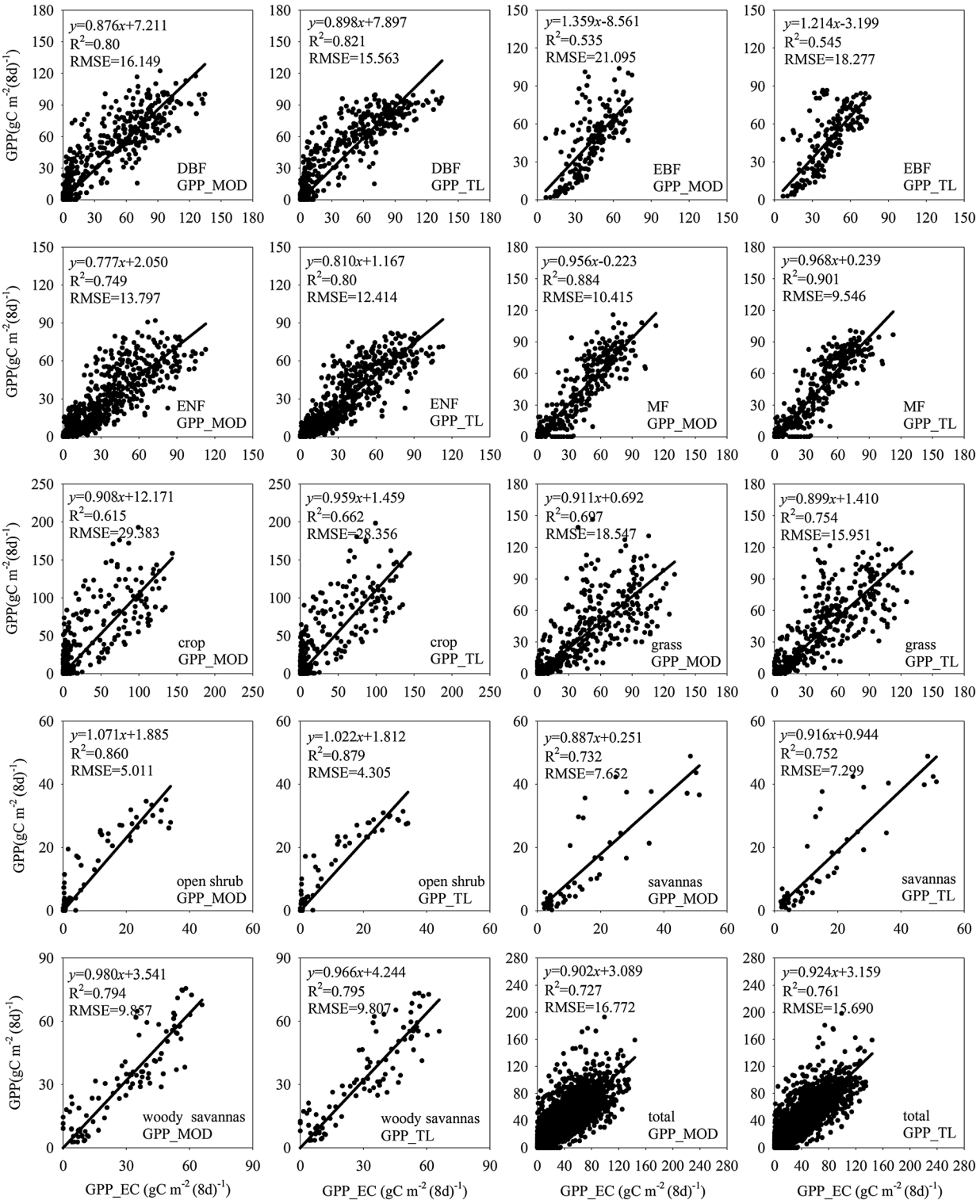

Figure 3. Validation of 8 day GPP calculated using the MOD17 (GPP_MOD) and TL-LUE (GPP_TL) models with corresponding tower measurements (GPP_EC) at the validation site years. Both the MOD17 and TL-LUE models were driven using average optimized parameters for the different vegetation types, smoothed LAI, and tower-based meteorological data.

Table 2. R^2, RMSE, and AIC for MOD17 and TL-LUE Models in Calibration and Validation Site Years

	MOD17			TL-LUE			Difference		
Vegetation Type	R^2	RMSE (g C m^{-2} $(8d)^{-1}$)	AIC	R^2	RMSE (g C m^{-2} $(8d)^{-1}$)	AIC	ΔR^2	RMSE (g C m^{-2} $(8d)^{-1}$)	ΔAIC
Calibration									
DBF	0.88	12.61	4979.1	0.90	11.21	4750.6	0.02	−1.40	−228.5
EBF	0.75	15.87	3053.9	0.78	14.25	2937.3	0.03	−1.62	−116.6
ENF	0.84	11.46	17287.4	0.87	9.96	16295.6	0.03	−1.50	−991.8
MF	0.84	12.25	9844.3	0.86	11.08	9452.1	0.02	−1.17	−392.2
Crop	0.82	20.19	4149.2	0.82	19.69	4116.6	0.00	−0.50	−32.6
Grass	0.81	11.84	5775.8	0.83	11.01	5606.5	0.02	−0.84	−169.2
OS	0.79	5.02	1041.0	0.84	4.48	969.8	0.05	−0.54	−71.3
S	0.64	12.20	692.4	0.72	10.67	657.4	0.08	−1.53	−35.0
WS	0.82	7.11	1084.7	0.87	5.97	990.3	0.05	−1.14	−94.5
Validation									
DBF	0.81	16.13	3144.1	0.83	15.49	3100.7	0.02	−0.64	−43.4
EBF	0.54	21.10	1124.0	0.55	18.28	1073.3	0.02	−2.82	−50.8
ENF	0.75	13.80	4621.0	0.80	12.41	4437.1	0.05	−1.38	−183.9
MF	0.88	10.42	2364.0	0.90	9.55	2278.2	0.02	−0.87	−85.8
Crop	0.62	29.38	2111.4	0.66	28.36	2091.2	0.04	−1.03	−20.2
Grass	0.70	18.55	3226.0	0.75	15.95	3061.6	0.05	−2.60	−164.5
OS	0.86	5.01	298.6	0.88	4.31	272.6	0.02	−0.71	−25.9
S	0.73	7.65	189.2	0.75	7.30	186.9	0.02	−0.35	−2.3
WS	0.79	9.86	423.0	0.80	9.81	424.1	0.01	−0.05	1.1

ΔR^2 means R^2 of GPP_TL minus that of GPP_MOD; ΔRMSE means RMSE of GPP_TL minus that of GPP_MOD; ΔAIC means AIC of GPP_TL minus that of GPP_MOD.
DBF: deciduous broadleaf forest; ENF: evergreen needleleaf forest; EBF: evergreen broadleaf forest; MF: mixed forest; Crop: crop; Grass: grass; S: savannas; OS: open shrub; WS: woody savannas.

technique and ecosystem respiration (Re) estimated using the Lloyd-Taylor equation [*Lloyd and Taylor*, 1994], which was fitted with the nighttime NEE data measured under turbulent conditions, i.e.,

$$R_e = R_{\text{ref}} e^{E_0\left(\frac{1}{(T_{\text{ref}}-T_0)}\frac{1}{(T-T_0)}\right)} \quad (1)$$

where R_{ref} represents the ecosystem respiration rate at a reference temperature (T_{ref}, 10°C); E_0 is the parameter that determines the temperature sensitivity of ecosystem respiration; T_0 is a constant and set to −46.02°C; and T is the air temperature or soil temperature (°C).

GPP is calculated as follows:

$$\text{GPP} = R_e - \text{NEE} \quad (2)$$

2.1.3. Leaf Area Index Data

The LAI was retrieved from the MODIS database and used to drive the two models. For each site, this database contains 8 day composite LAI values of pixels covering a 7 km × 7 km grid centered around the flux tower. Previous studies extracted LAI values averaged over the central 1 km × 1 km [*Yuan et al*., 2007], 3 km × 3 km [*Xiao et al*., 2008; *Schmid*, 2002], and 7 km × 7 km [*Groenendijk et al*., 2011] areas within the 7 km × 7 km cutouts to cover the flux tower footprint. Footprint modeling studies indicate that the area which contributes to the flux measured at eddy covariance flux towers varies from tens of meters to several kilometers [*Schmid*, 1997; *Chen et al*., 2012], normally about 20 to 100 times of the measurement heights. Therefore, in this study, as for crop, grass, savannas, open shrub, and woody savannas sites, LAI from the central 1 km × 1 km area was used since the corresponding measurement heights are mostly lower than 10 m. At the forest sites, LAI values averaged over the central 3 km × 3 km area were extracted since their measurement heights are mostly higher than 20 m. The resulting LAI time series for each site were further smoothed using the locally adjusted cubic-spline capping method [*Chen et al*., 2006] to remove unrealistically abrupt short-term changes in LAI due to the contamination of the measurements by clouds or the presence of ground snow or ice.

2.1.4. Albedo Data

The standard 8 day composite MODIS black-sky albedo product (MCD43A3) at 500 m gridded resolution [*Lucht et al*., 2000; *Schaaf et al*., 2002] was downloaded from the MODIS database (ftp://daac.ornl.gov/data/modis_ascii_subsets). Albedo averaged over the central 1 km × 1 km (for crop, grass, savannas, open shrub, and woody savannas) or

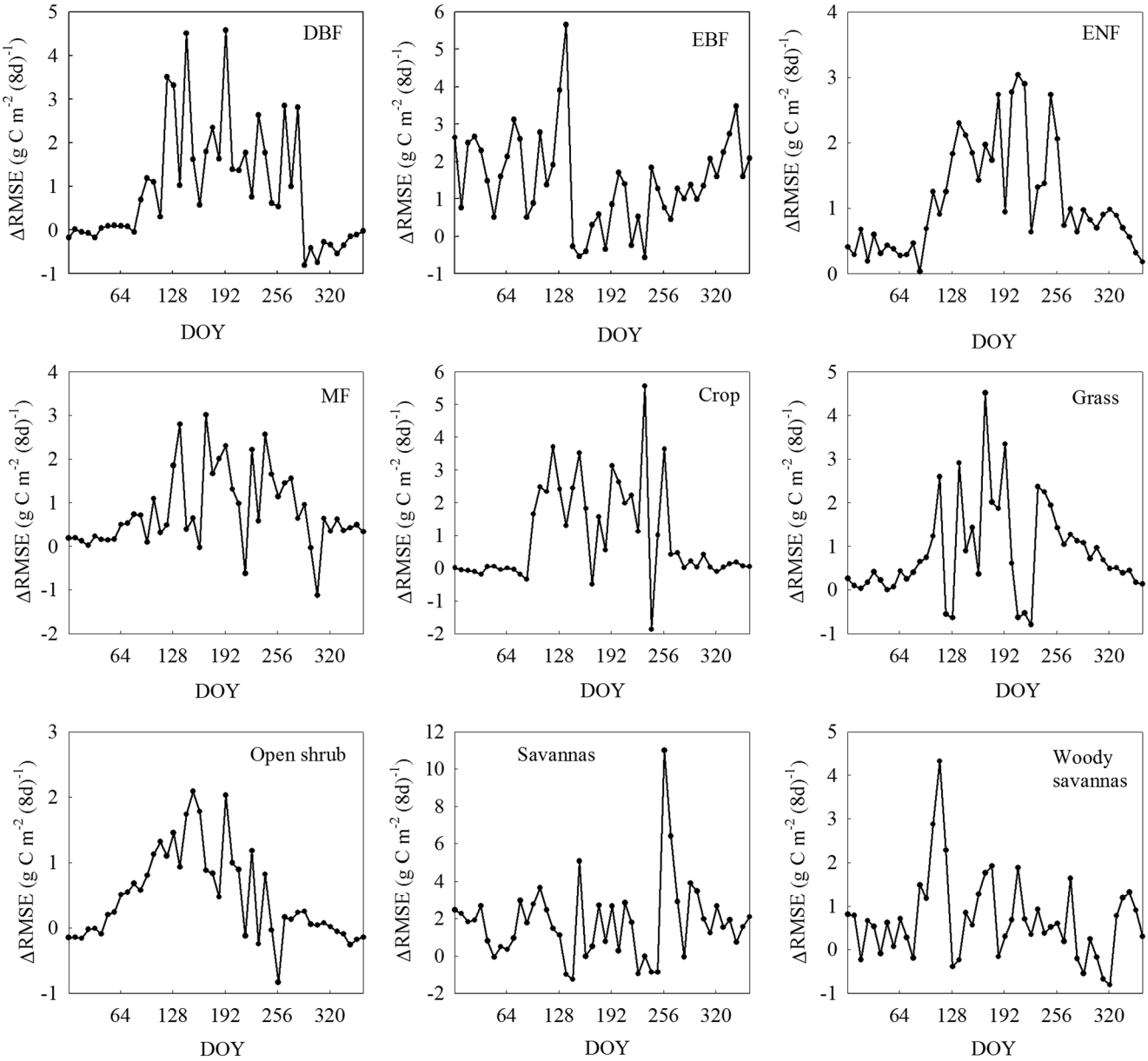

Figure 4. Seasonal dynamics of ΔRMSE over nine vegetation types. ΔRMSE means 8 day RMSE values of 8 day GPP_MOD against GPP_EC minus the corresponding values of GPP_TL against GPP_EC.

3 km × 3 km (for forests) area was used to drive the model. Outliers of MODIS albedo caused by clouds or the presence of ground snow or ice were filled using annual means.

2.2. The MOD17 GPP and TL-LUE Models

2.2.1. MODIS GPP Model

The MOD17 model is based on the radiation conversion efficiency concept of *Monteith* [1972] and the details are described in *Running et al.* [2000].

$$\mathrm{GPP} = \varepsilon_{\max} \times f(\mathrm{VPD}) \times g(T_{a\min}) \times \mathrm{PAR} \times f\mathrm{PAR} \quad (3)$$

where $\varepsilon_{\max}$ is the maximum light use efficiency and needs to be optimized; f(VPD) and $g(T_{\mathrm{amin}})$ are the scalars of VPD and minimum air temperature, respectively. fPAR is the fraction of PAR absorbed by the canopy and calculated as follows:

$$f\mathrm{PAR} = 1 - e^{-k \times \mathrm{LAI}} \quad (4)$$

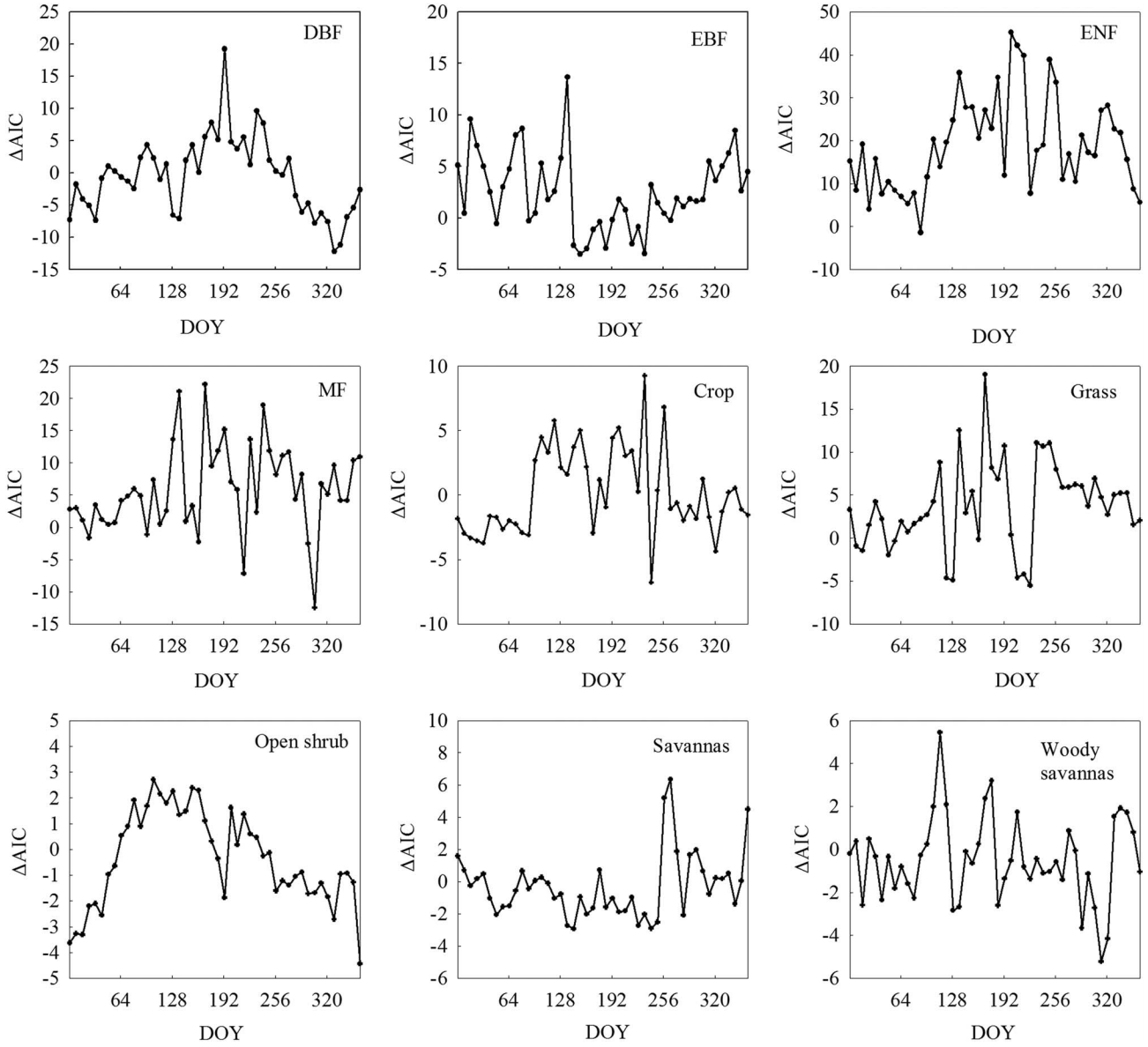

Figure 5. Seasonal dynamics of ΔAIC over nine vegetation types. ΔAIC means 8 day AIC values of 8 day GPP_MOD against GPP_EC minus the corresponding values of GPP_TL against GPP_EC.

In equation (3), $f(\mathrm{VPD})$ and $g(T_{\mathrm{amin}})$ are calculated as follows:

$$f(\mathrm{VPD}) = \begin{cases} 0 & \mathrm{VPD} \geq \mathrm{VPD}_{\max} \\ \dfrac{\mathrm{VPD}_{\max} - \mathrm{VPD}}{\mathrm{VPD}_{\max} - \mathrm{VPD}_{\min}} & \mathrm{VPD}_{\min} < \mathrm{VPD} < \mathrm{VPD}_{\max} \\ 1 & \mathrm{VPD} \leq \mathrm{VPD}_{\min} \end{cases} \quad (5)$$

$$g(T_{\mathrm{amin}}) = \begin{cases} 0 & T_{\mathrm{amin}} \leq T_{\mathrm{amin\,min}} \\ \dfrac{T_{\mathrm{amin}} - T_{\mathrm{amin\,min}}}{T_{\mathrm{amin\,max}} - T_{\mathrm{amin\,min}}} & T_{\mathrm{amin\,min}} < T_{\mathrm{amin}} < T_{\mathrm{amin\,max}} \\ 1 & T_{\mathrm{amin}} \geq T_{\mathrm{amin\,max}} \end{cases} \quad (6)$$

where $\mathrm{VPD}_{\max}$, $\mathrm{VPD}_{\min}$, $T_{\mathrm{amin\_max}}$, and $T_{\mathrm{amin\_min}}$ are parameters determined according to literature (Table 1).

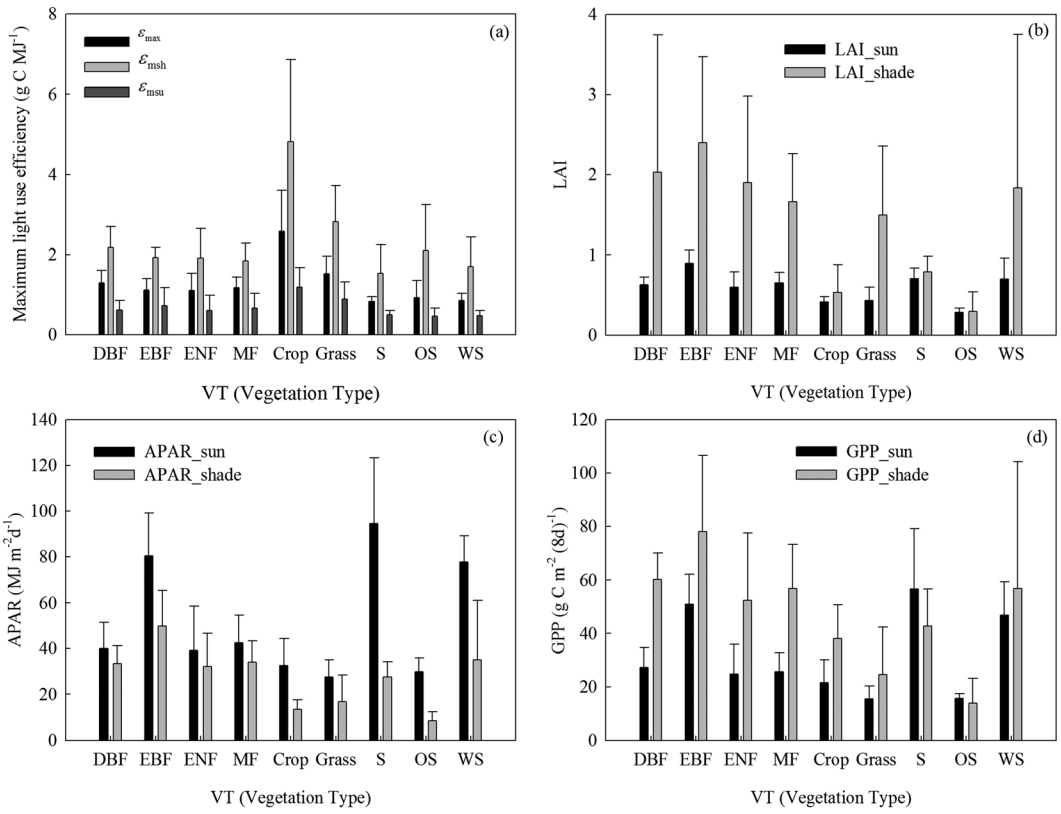

Figure 6. Mean annual values of optimized (a) maximum light use efficiency (ε_{max}), maximum light use efficiency of sunlit (ε_{msu}), and shaded (ε_{msh}) leaves, (b) LAI for sunlit and shaded leaves, (c) APAR for sunlit and shade leaves, and (d) simulated GPP for sunlit and shaded leaves for different vegetation types.

2.2.2. TL-LUE Model

The TL-LUE model developed by *He et al.* [2013] is stemmed from the MOD17 and BEPS models and calculates GPP of a plant canopy as follows:

$$\mathrm{GPP} = (\varepsilon_{msu} \times \mathrm{APAR}_{su} + \varepsilon_{msh} \times \mathrm{APAR}_{sh}) \times f(\mathrm{VPD}) \times g(T_{a\,min}) \quad (7)$$

where ε_{msu} and ε_{msh} are the maximum light use efficiency of sunlit and shaded leaves (which need to be optimized), respectively; APAR_{su} and APAR_{sh} are the PAR absorbed by sunlit and shaded leaves; f(VPD) and $g(T_{amin})$ are the scalars of VPD and minimum temperature, respectively, and also calculated using equations (5) and (6).

Table 3. Means, Standard Deviations (STDEV), and Coefficients of Variation (CV = STDEV/Means × 100%) of Optimized Maximum Light Use Efficiency (ε_{max}), Maximum Light Use Efficiency of Sunlit (ε_{msu}), and Shaded (ε_{msh}) Leaves for Different Vegetation Types

	Mean (g C MJ^{-1})			Standard Deviation (g C MJ^{-1})			CV (%)		
Vegetation Type[a]	ε_{max}	ε_{msh}	ε_{msu}	ε_{max}	ε_{msh}	ε_{msu}	ε_{max}	ε_{msh}	ε_{msu}
DBF	1.3	2.17	0.62	0.3	0.53	0.23	22.9	24.4	36.8
EBF	1.12	1.92	0.73	0.28	0.26	0.45	25.0	13.5	61.6
ENF	1.11	1.91	0.61	0.42	0.74	0.38	37.8	38.7	62.3
MF	1.18	1.84	0.66	0.26	0.44	0.38	22.0	23.9	57.6
Crop	2.58	4.81	1.19	1.02	2.05	0.49	39.4	42.7	41.2
Grass	1.52	2.82	0.89	0.44	0.9	0.43	28.9	31.9	48.3
Savannas	0.83	1.53	0.5	0.12	0.72	0.1	13.9	47.2	20
OS	0.93	2.11	0.46	0.42	1.13	0.21	45.6	53.5	45.3
WS	0.85	1.7	0.48	0.18	0.74	0.13	20.7	43.4	27.5

[a]DBF: deciduous broadleaf forest; ENF: evergreen needleleaf forest; EBF: evergreen broadleaf forest; MF: mixed forest; Crop: crop; Grass: grass; Savannas: savannas; OS: open shrub; WS: woody savannas.

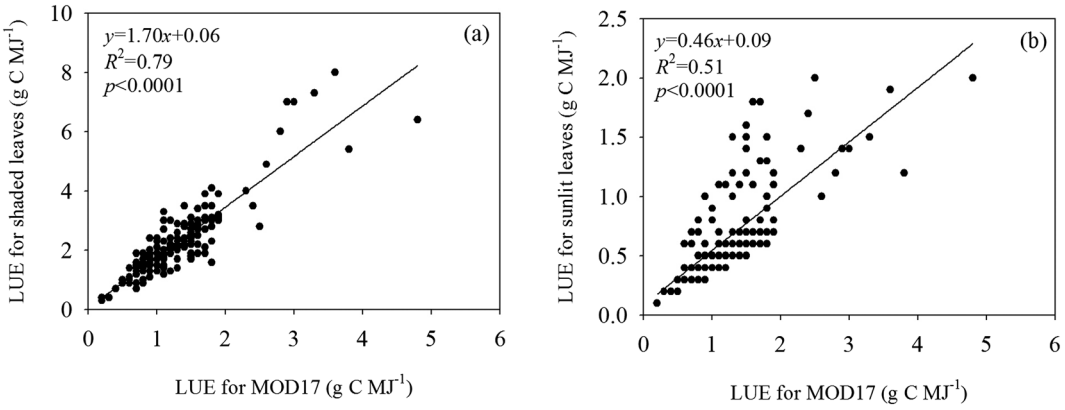

Figure 7. The linear relationships between ε_{max} and ε_{msh} and between ε_{max} and ε_{msu}.

$APAR_{su}$ and $APAR_{sh}$ in equation (7) are calculated as follows:

$$APAR_{su} = (1-\alpha)\times\left[PAR_{dir}\times\cos(\beta)/\cos(\theta) + \left(PAR_{dif} - PAR_{dif,u}\right)/LAI + C\right]\times LAI_{su} \quad (8)$$

and

$$APAR_{sh} = (1-\alpha)\times\left[\left(PAR_{dif} - PAR_{dif,u}\right)/LAI + C\right]\times LAI_{sh} \quad (9)$$

where α is the canopy albedo retrieved from the MODIS product; PAR_{dif} and PAR_{dir} are the diffuse and direct components of incoming PAR, respectively, and partitioned according to the clearness index [*Chen et al.*, 1999]; $PAR_{dif,u}$ is the diffuse PAR under the canopy and calculated following *Chen et al.* [1999]; (PAR_{dif}- $PAR_{dif,u}$)/LAI represents the diffuse PAR per unit leaf area within the canopy; *C* quantifies the contribution of multiple scattering of the total PAR to the diffuse irradiance per unit leaf area within the canopy; β is the mean leaf-sun angle and set as 60° for a canopy with a spherical leaf angle distribution; θ is the solar zenith angle[*Chen et al.*, 1999]; and LAI_{su} and LAI_{sh} are the LAI of sunlit and shaded leaves and are partitioned on the basis of LAI.

Diffuse and direct PAR can be empirically separated [*Chen et al.*, 1999; *Kathilankal et al.*, 2014]. In this study, they were partitioned following *Chen et al.* [1999] and with parameters calibrated using measured daily diffuse and total incoming radiation data [*He et al.*, 2013], i.e.,

$$PAR_{dif} = PAR\left(0.7527 + 3.8453R\text{-}16.316R^2 + 18.962R^3\text{-}7.0802R^4\right) \quad (10)$$

$$PAR_{dir} = PAR - PAR_{dif} \quad (11)$$

where PAR_{dif} represents the diffuse PAR; PAR is the total incoming photosynthetically active radiation, and *R* is the sky clearness index and equals PAR/($0.5S_0\cos\theta$); S_0 is the solar constant (1367 W m^{-2}). A constant 0.5 is used to convert incoming solar radiation into PAR [*Weiss and Norman*, 1985; *Tsubo and Walker*, 2005; *Bosch et al.*, 2009].

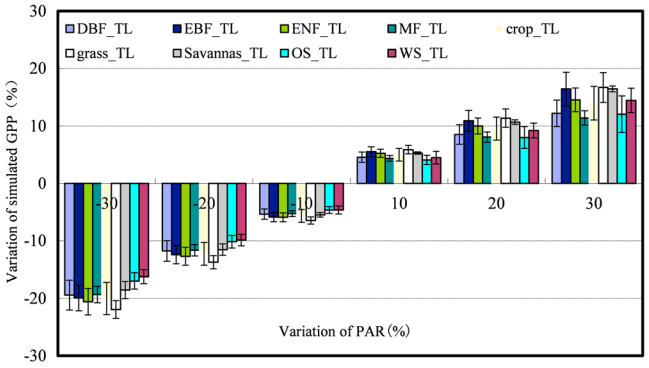

Figure 8. Sensitivity of GPP simulated by the MOD17 and TL-LUE models to PAR.

Direct and diffuse radiation measured simultaneously without continuous gaps in 37 sites years, including 22 sites and 7 vegetation types (Crop, DBF, EBF, ENF, MF, grass, and savannas), were used to validate the direct and diffuse radiation estimated using equations (10) and (11) (Table A3 in Appendix A). The estimated direct and diffuse PAR values were in good agreement with measurements with slopes of 0.98 and 0.97 and R^2 values

Table 4. Sensitivity of GPP Simulated by the MOD17 and TL-LUE Models to PAR[a]

	Variation of GPP_TL (%)								
Variation of PAR (%)	DBF	EBF	ENF	MF	Crop	Grass	Savannas	OS	WS
−30	−19.4	−19.9	−20.6	−19.3	−20.0	−21.9	−18.5	−17.0	−16.2
−20	−11.8	−12.4	−12.7	−11.7	−12.3	−13.7	−11.5	−10.2	−9.9
−10	−5.4	−5.9	−5.9	−5.3	−5.7	−6.5	−5.5	−4.6	−4.6
10	4.5	5.5	5.2	4.4	5.0	5.9	5.3	4.1	4.5
20	8.5	10.9	10.0	8.1	9.6	11.4	10.7	8.0	9.2
30	12.2	16.4	14.5	11.4	14.0	16.7	16.4	12.1	14.4

[a]DBF: deciduous broadleaf forest; ENF: evergreen needleleaf forest; EBF: evergreen broadleaf forest; MF: mixed forest; Grass: grass; Crop: crop; Savannas: Savannas; OS: open shrub; WS: woody savannas.

of 0.94 and 0.84, respectively. The root-mean-square error (RMSE) of estimated daily direct and diffused PAR against observed values were 0.64 and 0.61 MJ m^{-2} d^{-1}, respectively (Figure 1).

LAI_{su} and LAI_{sh} were partitioned as follows:

$$LAI_{sum} = 2\times\cos(\theta)\times\left(1-\exp\left(-0.5\times\Omega\times\frac{LAI}{\cos(\theta)}\right)\right) \quad (12)$$

$$LAI_{sh} = LAI - LAI_{su} \quad (13)$$

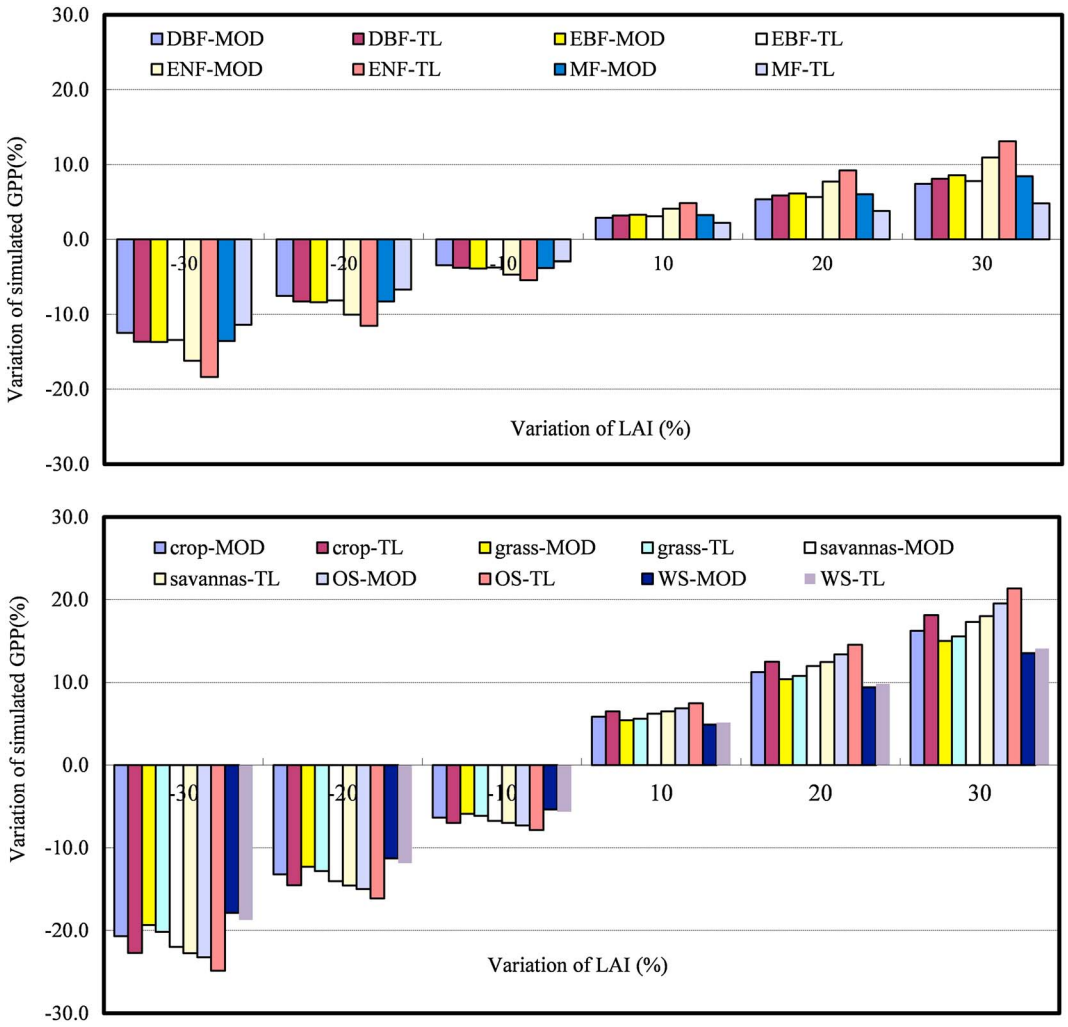

Figure 9. Sensitivity of GPP simulated by the MOD17 and TL-LUE models to LAI.

Table 5. Sensitivity of GPP Simulated by the MOD17 and TL-LUE Models to LAI[a]

Variation of LAI (%)	Variation of GPP_MOD (%)							Variation of GPP_TL (%)						
	DBF	EBF	ENF	MF	Crop	Grass	Savannas	OS	WS	DBF	EBF	ENF	MF	Crop	Grass	Savannas	OS	WS
−30	−12.5	−13.7	−16.2	−13.6	−19.3	−19.3	−22.0	−23.2	−17.9	13.7	−13.4	−18.4	−11.4	−22.7	−20.2	−22.7	−24.9	−18.7
−20	−7.5	−8.4	−10.0	−8.3	−12.3	−12.3	−14.0	−15.0	−11.3	−8.3	−8.1	−11.5	−6.7	−14.5	−12.8	−14.6	−16.1	−11.9
−10	−3.4	−3.8	−4.7	−3.8	−5.9	−5.9	−6.7	−7.3	−5.4	−3.8	−3.7	−5.4	−2.9	−7.0	−6.1	−7.0	−7.9	−5.6
10	2.9	3.3	4.1	3.2	5.4	5.4	6.2	6.9	4.9	3.2	3.1	4.9	2.2	6.5	5.6	6.5	7.5	5.1
20	5.3	6.1	7.7	6.0	10.4	10.4	12.0	13.4	9.4	5.9	5.7	9.2	3.8	12.5	10.8	12.5	14.6	9.8
30	7.4	8.6	10.9	8.4	15.0	15.0	17.3	19.6	13.6	8.1	7.8	13.1	4.8	18.1	15.6	18.0	21.3	14.1

[a]DBF: deciduous broadleaf forest; ENF: evergreen needleleaf forest; EBF: evergreen broadleaf forest; MF: mixed forest; Grass: grass; Crop: crop; savannas: savannas; OS: open shrub; WS: woody savannas.

where θ is the solar zenith angle [*Chen et al.*, 1999]; LAI is the total leaf area index of the canopy; and Ω was the clumping index according to Table 1.

2.3. Model Parameterization and Validation

Maximum LUE for the whole canopy in the MOD17 algorithm (ε_{max}) and for sunlit leaves (ε_{msu}) and shaded leaves (ε_{msh}) in the TL-LUE model was optimized using measured GPP values in 195 site years. The optimization was implemented using the shuffled complex evolution-University of Arizona method [*Duan et al.*, 1992]. Both MODIS and TL-LUE models were driven by 8 day VPD, T_a, PAR, and LAI. The ε_{max}, ε_{msu}, and ε_{msh} were annually optimized for each site year. In the optimization, model performance was evaluated using the agreement index (d), which is defined as follows:

$$d = 1 - \sum_{k=1}^{n} (P_k - O_k)^2 / \sum_{k=1}^{n} (|P_k - \overline{O}| + |O_k - \overline{O}|)^2 \quad (14)$$

where n is the total number of measurements; P_k and O_k represent the kth predicted and observed 8 day GPP values, respectively, and $\bar{O}$ is the annual mean of observed GPP values.

The relationship of d with the root-mean-square error (RMSE) and the correlation coefficient (R) is as follows:

$$d = 1 - \frac{(\mathrm{RMSE})^2}{\sigma_{OP}^2 + \sigma_P^2 + 2|R\sigma_{OP}\sigma_P|} \quad (15)$$

where $\sigma_{OP}^2 = \sum_{i=1}^{n} (P_i - \overline{O})^2$, $\sigma_P^2 = \sum_{i=1}^{n} (O_i - \overline{O})^2$.

The index d can synthesize the information contained in RMSE, R^2, σ_{OP}, and σ_P. It has the advantage of being both relative, as opposed to R^2, and bounded in the range from 0 (no agreement) to 1 (complete agreement), as opposed to RMSE [*Willmott*, 1981, 1982]. This index has been widely utilized in model parameter optimization [*Wang et al.*, 2001; *Gu et al.*, 2002].

2.4. Model Performance Assessment

The performance of TL-LUE and MOD17 was assessed using the root-mean-square error (RMSE), the coefficient of determination (R^2), and the Akaike information criterion (AIC). AIC has the advantage of testing the significance of the differences between the functions of different model specifications [*Wang and Liu*, 2006] and measuring the parameters of a model [*Akaike*, 1974]. It is defined as follows:

$$\mathrm{AIC}(p) = N \log E(p) + 2p \quad (16)$$

where p is the order of model, N the number of data, and $E(p)$ innovation variance. The AIC best model has the smallest AIC value [*Inouye et al.*, 1995; *Harada et al.*, 2010].

3. Results

3.1. Performance of MOD17 and TL-LUE

Figure 2 shows the comparison of GPP simulated using the MOD17 model (GPP_MOD) and TL-LUE model (GPP_TL) against GPP_EC in 195 calibration site years for all nine VTs. Both simulated GPP_MOD and GPP_TL were in good agreement with GPP_EC. When the data

from the 195 site years were lumped together, R^2 and RMSE values for GPP_MOD were 0.83 and 12.84 gC m^{-2} (8d)$^{-1}$, respectively, and the corresponding values for GPP_TL were 0.86 and 11.79 gC m^{-2} (8d)$^{-1}$. When analyzed for individual VTs, the R^2 and RMSE for GPP_MOD versus GPP_EC ranged from 0.64 for savannas to 0.88 for deciduous broadleaf forests and from 5.02 gC m^{-2} (8d)$^{-1}$ for open shrub vegetation to 20.19 gC m^{-2} (8d)$^{-1}$ for crops, respectively. The corresponding values of GPP_TL were in the range from 0.72 for savannas to 0.90 for deciduous broadleaf forests and from 4.48 gC m^{-2} (8d)$^{-1}$for open shrub to 19.69 gC m^{-2} (8d)$^{-1}$ for crops, respectively.

Using optimized ε_{max}, ε_{msu}, and ε_{msh} values, simulated and measured GPP values for the 73 validation site years are compared for individual VTs in Figure 3. When all VTs were lumped together, variations of 8 day GPP explained by the MOD17 and TL-LUE models were 72.7% and 76.1%, respectively. The corresponding RMSE values were 16.77 gC m^{-2} (8d)$^{-1}$ and 15.69 gC m^{-2} (8d)$^{-1}$. The TL-LUE model produced higher R^2 and lower RMSE values than the MOD17 model for all VTs. The improvement of GPP estimated with TL-LUE over that estimated with the MOD17 model was most significant for grass and ENF, with R^2 increased from 0.70 to 0.75 for grass and from 0.75 to 0.80 for ENF. The corresponding RMSE decreased from 18.55 gC m^{-2} (8d)$^{-1}$ to 15.95 gC m^{-2} (8d)$^{-1}$ for the former and from 13.80 gC m^{-2} (8d)$^{-1}$ to 12.41 gC m^{-2} (8d)$^{-1}$ for the latter.

Out of the total of 195 calibration years, R^2 values of GPP_TL against measurements were higher than those of GPP_MOD in 172 (88%) site years. The RMSE values of GPP_TL were smaller than those of GPP_MOD in 184 (94%) site years. The AIC values of GPP_TL were lower than those of GPP_MOD for all VTs, especially for ENF, grass, and MF (Table 2). Out of the total of 73 validation years, the TL-LUE model outperformed the MOD17 model in 67 (92%) of site years according to R^2 of simulated GPP and in 61 (84%) site years according to RMSE of simulated GPP. The AIC values of GPP_TL were lower than those of GPP_MOD for all vegetation types but woody savannas (Table 2).

Figure 4 presents the seasonal variations of RMSEs of 8 day GPP_TL and GPP_MOD against GPP_EC. The RMSE values of GPP_TL were almost smaller than those of GPP_MOD in all seasons for all vegetation types. The decrease of RMSE of GPP_TL relative to that of GPP_MOD was more obvious during the growing season for all vegetation types but savannas and woody savanna. As to DBF, MF, crop, and grass, the AIC values of 8 day GPP_TL were lower than those of the 8 day GPP_MOD product during the growing season with high GPP, indicating the robust outperformance of the TL-LUE model over the MOD17 model (Figure 5). During off-season periods with low GPP, the AIC values of GPP_TL were slightly higher than those of GPP_MOD. As to ENF and EBF, the TL-LUE model performed better than the MOD17 model in all seasons, which is confirmed by the lower AIC values of the former. As indicated by slightly higher AIC values, the outperformance of TL-LUE over MOD17 was not significant for open shrub, savannas, and woody savannas.

3.2. Optimized Maximum Light Use Efficiency

Figure 6a and Table 3 show the averages of the optimized ε_{max} values in the MOD17 model, as well as ε_{msu} and ε_{msh} in the TL-LUE model for nine VTs. The values of these parameters varied substantially among the different vegetation types. For all VTs, values of ε_{msh} were always the highest and those of ε_{msu} were the lowest with the values of ε_{max} in between. As expected, crop had the highest ε_{max}, ε_{msh}, and ε_{msu} values, which were 2.58, 4.81, and 1.19 gC MJ^{-1}, respectively. The ε_{max}, ε_{msh}, and ε_{msu} values of savannas were only 0.83, 1.53, and 0.50 gC MJ^{-1} and were lower than those of all other VTs. For a given plant function type, ε_{max}, ε_{msh}, and ε_{msu}, all exhibited considerable variations among different site years. The coefficients of variations (CV = standard deviation/mean × 100%) for ε_{max}, ε_{msh}, and ε_{msu} ranged from 13.9% for savannas to 45.6% for open shrub, from 13.5% for EBF to 53.5% for open shrub, and from 20.0% for savannas to 62.3% for ENF, respectively. Figure 7 shows that there were tight linear relationships between ε_{max} (denoted as x, gC MJ^{-1}) with ε_{msh} (denoted as y_1, gC MJ^{-1}) and between ε_{max} with ε_{msu} (denoted as y_2, gC MJ^{-1}), which were described as $y_1 = 1.70x + 0.06$ ($R^2 = 0.79$, $p < 0.0001$) and $y_2 = 0.46x + 0.09$ ($R^2 = 0.51$, $p < 0.0001$). ε_{msh} was 2.63 to 4.59 times ε_{msu}.

Figures 6b–6d show the averages and standard deviations of LAI, APAR, and GPP of sunlit and shaded leaves calculated by the TL-LUE model for the nine vegetation types. The values varied distinctively among the different vegetation types. The ratio of shaded LAI to sunlit LAI ranged from 1.06 for open shrub to 3.22 for DBF. As expected, the APAR of shaded leaves was much lower than that of sunlit leaves. The ratio of the former to the latter ranged from 0.28 for open shrub and to 0.84 for DBF. The GPP of shaded leaves was much higher than that of sunlit leaves for most vegetation types with the exception of savannas and open shrub. The

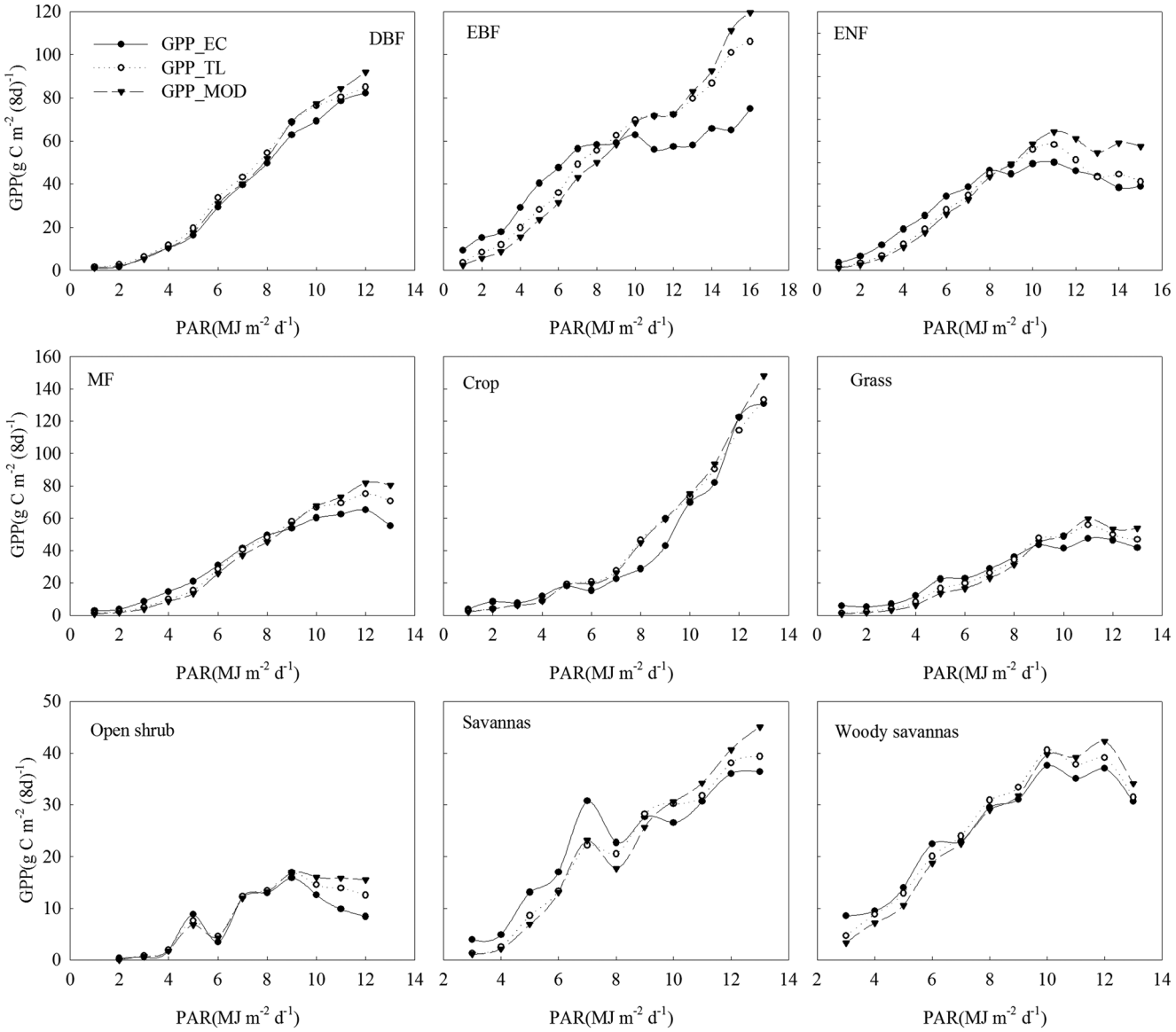

Figure 10. Effects of varying PAR on GPP simulated using the TL-LUE and MOD17 models.

ratio of GPP of shaded leaves to and that of sunlit leaves ranged from 0.75 for savannas to 2.22 for DBF. The higher GPP of shaded leaves results mainly from their higher maximum light use efficiency (ε_{msh}) and larger LAI.

3.3. Sensitivity of GPP Simulation to PAR and LAI Driving MOD17 and TL-LUE Models

The sensitivity of simulated GPP to PAR and LAI was assessed through artificial variations of these two variables by ±30%, ±20%, and ±10%. The variations of PAR were partitioned into the variations of direct and diffuse components according to the sky clearness index (R) using equations (10) and (11), and LAI variations were partitioned into variations of sunlit and shaded LAI according to solar zenith angle using equations (12) and (13). GPP_TL showed a weaker sensitivity to variations in PAR than GPP_MOD (Figure 8 and Table 4). An increase in PAR by 10%, 20%, and 30% resulted in an overestimate of GPP_TL in the range from 4.1%, 8.0% for OS, and 11.4% for MF to 5.9%, 11.4%, and 16.7% for grass, respectively. A decrease in PAR by 10%, 20%, and 30% resulted in an underestimate of GPP_TL in the range from 4.6%, 9.9%, and 16.2% for WS to 6.5%, 13.7%, and 21.9% for grass, respectively. In contrast, the change in GPP simulated by the MOD17

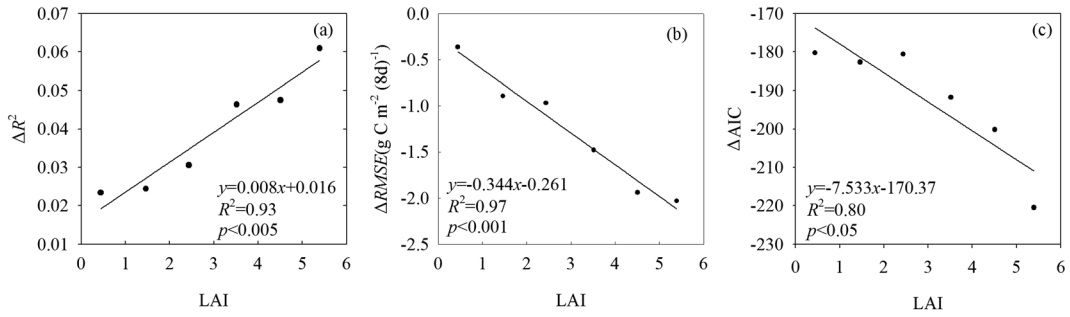

Figure 11. Changes of (a) R^2 and (b) RMSE of GPP_TL versus GPP_EC minus the corresponding values of GPP_MOD with LAI.

model was equal to the change in PAR. The sensitivity of simulated GPP_TL to LAI was slightly higher (no more than 2%) than that of GPP_MOD (Figure 9 and Table 5).

In order to further analyze the sensitivity of simulated GPP to PAR for different vegetation types under different conditions of incoming PAR, observed and simulated GPP were averaged over 1 MJ m^{-2} d^{-1} bins of PAR. Both the TL-LUE and MOD17 models tended to underestimate GPP when PAR was low and overestimate GPP when PAR was high (Figure 10). GPP_TL deviated less from GPP_EC than GPP_MOD. With the increase of PAR, the departure of GPP_TL from GPP_EC became much smaller than that of GPP_MOD.

Figure 11 shows the changes of R^2, RMSE, and AIC of GPP_TL against GPP_EC minus the corresponding values of GPP_MOD with LAI. The higher the LAI, the higher values of ΔR^2 and absolute ΔRMSE and ΔAIC. It means that with the increase of LAI, the TL-LUE model outperformed the MOD17 model more significantly. This would be one of the reasons that in both calibration and validation, the RMSE values of GPP_TL were lower than that of GPP_MOD in growing seasons than in nongrowing seasons (Figure 4). LAI is much higher in growing seasons than in nongrowing seasons. The result is consistent with the findings of *Knohl and Baldocchi* [2008] and *Wohlfahrt et al*. [2008].

4. Discussions

4.1. Improvement of the TL-LUE Model Over the MOD17 Model

The comparison of RMSE and AIC of GPP_TL against GPP_EC with those of GPP_MOD indicates that the improvement of TL-LUE model over the MOD17 model is more significant during the growing season compared to off-season periods (Figures 4 and 5). One factor resulting in the seasonal change in the improvement of TL-LUE model over the MOD17 model is the seasonal variations of LAI, especially for nonevergreen vegetation. When LAI is low, the canopy consists dominantly of sunlit leaves, which are the main contributor to the canopy GPP. So the TL-LUE and MOD17 model perform similarly. With the increase of LAI, shaded leaves make a large contribution to canopy GPP. As a consequence, the outperformance of TL-LUE over MOD17 became considerable. The ΔR^2 (R^2 of GPP_TL against GPP_EC minus the corresponding value of GPP_MOD) increased significantly, while ΔRMSE and ΔAIC (RMSE and AIC of GPP_TL against GPP_EC minus the corresponding values of GPP_MOD) decreased significantly (Figure 11). Similar findings were also reported in *Wohlfahrt et al*. [2008].

During the growing season, incoming PAR varied across a wider range. When incoming PAR is high, direct PAR is dominant and absorbed by sunlit leaves, which are commonly light saturated. Consequently, the LUE of the whole canopy is low [*Gu et al*., 2002; *Ibrom et al*., 2008]. Under the condition of low PAR, the fraction of diffuse PAR is high and uniformly distributed within the canopy. A larger part of the incoming PAR will be absorbed by shaded leaves. Their photosynthesis is commonly light limited and might be significantly enhanced by increasing PAR. Therefore, the LUE of whole canopy is high [*Zhang et al*., 2011]. The MOD17 model ignores the change of LUE with incoming PAR and definitely overestimates/underestimates GPP when incoming PAR is high/low. The TL-LUE model differentiates ε_{msu} and ε_{msh} and properly captures the change in fraction of incoming PAR absorbed by sunlit and shaded leaves [*He et al*., 2013]. It is able to alleviate the bias in GPP simulated by the MOD17 model.

Observed incoming PAR data are very limited. Currently, PAR used to simulate regional and global GPP is generated from model simulations, remote sensing, and data assimilation. Many studies have indicated that large uncertainties exist in these data sets. For example, *Zhao and Running* [2006] pointed out that the average bias of NCEP area-weighted radiation was about 20%. Also, based on field measurements, *Betts et al*. [1996] and *Brotzge* [2004] showed that shortwave solar radiation was consistently overestimated by 17–27% in the NCEP-NCAR data set. With a data set of daily and monthly solar radiation from ground observations at 122 stations over China using thermopile pyranometers, *Jia et al*. [2013] found that in the reanalyzed data (NCEP-DOE), shortwave solar radiation was greatly overestimated in China, especially in north and south regions, with mean bias errors of 32.1% and 31.9%, respectively. GPP_TL exhibited a much lower sensitivity to PAR than GPP_MOD (Figure 8). An overestimate of 30% in incoming PAR resulted in an averaged overestimation of GPP_TL in the range from 13.3% (grass) to 18.6% (MF), much smaller that the overestimation of 30% in GPP_MOD. Similarity, the underestimation of GPP_TL caused by a negative bias of incoming PAR was also smaller than that of GPP_MOD. If incoming PAR consisted solely of direct or diffuse beams, the sensitivity of GPP_TL to incoming PAR would be the same as that of GPP_MOD.

In the TL-LUE model, PAR is partitioned into direct and diffuse components. The former is absorbed only by sunlit leaves, while the latter can be utilized by both sunlit and shaded leaves. Owing to large difference between ε_{msu} and ε_{msh}, the errors in the partitioning of direct and diffuse PAR will definitely propagate into simulated GPP. The validation in 37 sites years showed that the RMSE of estimated diffused PAR against observations was 0.61 MJ m^{-2} d^{-1}. In the case of extreme underestimation of diffuse PAR, the relative error of GPP_TL would be 6.2%. The extreme overestimation of diffuse PAR would induce an overestimation of 10.9% in GPP_TL. Compared with the MOD17 model, the requirement for partitioning PAR into direct and diffuse components is a disadvantage of the TL-LUE model. However, this shortcoming is overwhelmed by the advantage of the low sensitivity of the TL-LUE model to uncertainties in incoming PAR. The average 6.2%/10.9% underestimation/overestimation in GPP_TL caused by an extreme underestimation/overestimation of diffuse PAR was smaller than the average 8.1% (=30% − 21.9%) /13.3% (=30% − 16.7%) reduction of underestimation/overestimation in GPP_TL relative to GPP_MOD caused by a 30% underestimation/overestimation of PAR (Table 4).

4.2. The Optimized Maximum Light Use Efficiency

The optimized ε_{msh} was much higher than ε_{max} and ε_{msu}. Open shrub had the highest ratio of ε_{msh} to ε_{msu} (4.59) and EBF the lowest (2.63). Higher ε_{msh} can be attributed to the fact that shaded leaves only have the opportunity to absorb diffuse light (including the incoming diffuse sunlight reaching to the canopy and the multi-scattered direct sunlight in the canopy), which enters the plant canopy from all directions and reaches leaves more evenly than direct light [*Sinclair et al*., 1992; *Hammer and Wright*, 1994]. The intensity of light absorbed by shaded leaves varies normally in the almost linear part of the light response curve that lies between the light compensation point and the light saturation point, which is the reason for their higher light use efficiency compared to sunlit leaves. The differentiation of ε_{msh} and ε_{msu} enables the TL-LUE model to simulate the enhanced effect of diffuse radiation on LUE [*He et al*., 2013], which has been previously reported for crop and grass [*Sinclair et al*., 1992; *Sinclair and Shiraiwa*, 1993; *Rochette et al*., 1996; *Gu et al*., 2002; *Wohlfahrt et al*., 2008] and coniferous and deciduous forests [*Price and Black*, 1990; *Hollinger et al*., 1994; *Baldocchi*, 1997; *Goulden et al*., 1997; *Lamaud et al*., 1997; *Freedman et al*., 2001; *Ibrom et al*., 2006]. Globally, irradiance over land surfaces declined by an average of 20 Wm^{-2} over the past 50 years [*Stanhill and Cohen*, 2001], especially during 1960–1999 [*Mercado et al*., 2009], while aerosol concentrations and cloudiness might result in increase of diffuse radiation. With the consideration of the enhancing effect of diffuse irradiance on GPP, the TL-LUE model might be used to simulate the impact of the changes in diffuse to global radiation ratio on GPP.

The average optimized ε_{max} was close to the default values used in the MOD17 model (Table 1) for all VTs with the exception of crop and grass, which exhibited much higher optimized ε_{max} values than the default (0.604 gC MJ^{-1} PAR). Many studies indicated that the underestimation of GPP for crop by the MOD17 model is mainly due to using a too low value of ε_{max} [*Turner et al*., 2006]. It has been reported that the mean LUE of crop can approach 2.80 gC MJ^{-1} PAR [*Garbulsky et al*., 2010; *Xiao et al*., 2011; *Chen et al*., 2011], which is slightly higher than the average value of 2.58 gC MJ^{-1} PAR optimized here. The optimized ε_{max} of grass averaged 1.52 g C MJ^{-1} (from 1.0 gC MJ^{-1} to 2.5 gC MJ^{-1}), much higher than the value of 0.604 gC MJ^{-1} used in MOD17 model. *Sjöström et al*. [2013] also found a significant improvement in simulating GPP of grass if ε_{max}

was set to 1.7 gC MJ^{-1}. The higher ε_{max} for crop and grass is probably related to fertilization and the increased use of productive and C_4 plants with higher water use efficiencies, respectively.

There were tight linear relationships of ε_{msh} and ε_{msu} with ε_{max}, e.g., ε_{msh} was about 1.70 times ε_{max}, and ε_{msu} only about 0.46 times ε_{max} (Figure 7). These relationships are relatively strict and may be used for a quick estimation of ε_{msh} and ε_{msu} values from existing ε_{max} values. These robust and relatively constant relationships between the different LUE estimators indicate that there is a similar functional pattern across different biomes in the way how diffuse and direct radiation are used for GPP. The empirical, functional parameter estimation approach does however not distinguish between the different reasons for the observed patterns, which can be caused by shade modification of leaf physiology but as well by differences in PAR absorptivity, leaf angle distributions, canopy structure, and the distribution of shade and sunlit leaves across the plant canopy. The results show similarities in the ways canopies utilize diffuse and direct radiation, not how they achieve this.

Some LUE models apply a universally invariant LUE values for various ecosystems. For example, the C-Fix model assumed a value of 1.1 g C m^{-2} MJ^{-1} APAR for all vegetation types [*Veroustraete et al.*, 2002]. In the EC-LUE model, LUE equals 2.14 g C m^{-2} MJ^{-1} APAR without biome-dependent variations across biomes [*Yuan et al.*, 2007]. This study found out that ε_{max}, ε_{msh}, and ε_{msu} varied considerably not only among different VTs but also across different sites within a specific VT. Such variation has been previously reported in many studies [*Russell et al.*, 1989; *Groenendijk et al.*, 2011]. The variations of ε_{max}, ε_{msh}, and ε_{msu} across different sites might be caused by a number of factors, including plant species, forest age, nitrogen content of leaves, and fraction of diffuse radiation. These factors have not been included yet in MOD17 and TL-LUE models, suggesting the necessity of further improving their parameterization for a better simulation of GPP. The inclusion of the changes in LUE with the above mentioned factors will further improve the ability of LUE models to simulate GPP.

4.3. Uncertainties

LAI is an input into the MOD17 and TL-LUE models. Simulated GPP is affected by the quality of LAI, which might be extracted from literature for these sites used in this study. However, only average or maximum LAI values are typically reported [*Heinsch et al.*, 2006]. In reality, LAI varies seasonally, even for evergreen forests. Therefore, MODIS LAI rather than measured LAI was used in this study to drive the models for optimizing ε_{max}, ε_{msh}, and ε_{msu}. Such simple application of MODIS LAI might induce some uncertainties in optimized parameters and GPP validation. First, MODIS LAI usually has an error of about 20% [*Fang et al.*, 2012], which definitely propagate into optimized parameters and estimated GPP. Sensitivity analysis showed that 20% of error in LAI may cause detectable errors in calculated GPP (Figure 9), ranging from 5.3% to 7.7% for forest and 9.4% to 13.4% for other VTs for the MOD17 model and 3.8% to 9.2% for forests and from 9.2% to 14.6% for other VTs for the TL-LUE model. Additionally, the mismatch of the spatial resolution of MODIS LAI with the footprints of eddy covariance flux towers might also bring some uncertainties in parameter parameterization and GPP simulation. Furthermore, the vegetation type around many FLUXNET towers is not completely homogenous. MODIS LAI from pixels around towers might not actually represent the LAI of various types of vegetation with different maximum light use efficiency, namely, even the 1 km MODIS pixel does not represent what the flux tower measured. *Román et al.* [2009] developed a method to quantify the representativeness of MODIS pixels for tower comparisons. Unfortunately, their analysis has not been conducted for all FLUXNET sites used in this study. In future, high spatial and temporal resolution LAI data should be used in conjunction with footprint models to constrain uncertainties in parameter optimization and GPP estimation caused vegetation heterogeneity.

Generally, VPD and T_a have been used to represent the environmental controls on GPP. VPD represents part of the atmospheric evaporative demand and its effect on photosynthesis and was shown to be one of the key factors reducing LUE [*Gu et al.*, 2002; *Lloyd et al.*, 2002; *Yuan et al.*, 2007; *Ibrom et al.*, 2008]. Some previous studies have also outlined the important role of soil moisture in regulating LUE and GPP [*Jarvis and Linder*, 2000; *Xu and Baldocchi*, 2004; *Baldocchi et al.*, 2005; *Yuan et al.*, 2007]. The exclusion of soil moisture in the TL-LUE and MOD17 models may have induced some uncertainties in optimized parameters and calculated GPP, as is evident in the somewhat poor agreement of observed and simulated GPP for open shrub, savannas, and woody savannas, in which soil water stress is likely to occur frequently. Soil moisture maybe included into the TL-LUE models via the Soil Moisture Active and Passive and Soil Moisture and Ocean Salinity satellite data in the future.

As sunlit leaves received both direct and diffuse radiation, they are supposed to have higher temperature than shaded leaves, which may lead to greater temperature gradients between sunlit leaves and the

surrounding air. It means that the scalars (equations (5) and (6)) should be calculated using different temperatures for sunlit and shaded leaves. The TL-LUE model presently takes the same air temperature to calculate temperature scalars for sunlit and shaded leaves. Additionally, differences in leaf temperature can also result in different VPD of sunlit and shaded leaves. In the TL-LUE and MOD17 models, the application of same temperature and VPD for entire canopy might be also a source of uncertainties in simulated GPP and optimized parameters. In addition, flux data from a limited number of savannas, open shrubs, and woody savannas were used to optimize parameters and assess model performance, which makes conclusions more uncertain.

5. Conclusions

In this study, the TL-LUE model was optimized and validated using global FLUXNET CO_2 flux measurements. The performance of the model was compared with that of the widely used MOD17 model. The main conclusions are as follows:

1. The TL-LUE model outperformed the MOD17 model in simulating 8 day GPP. The improvement of the TL-LUE model over the MOD17 model became more apparent at higher LAI.
2. Optimized ε_{max}, ε_{msu}, and ε_{msh} varied considerably among VTs and across different sites for a specific VT. Values of ε_{msh} and ε_{msu} were linearly correlated with the values of ε_{max}. ε_{msh} was about 1.70 times ε_{max}, and ε_{msu} about 0.46 times ε_{max}. The average values of optimized ε_{max} were close to the default values used in the MOD17 algorithm for all VTs except crop and grass. For the latter two VTs, optimized ε_{max} values were much larger than the default values used in the MOD17 algorithm.
3. GPP simulated by the TL-LUE and the MOD17 models showed a similar sensitivity to LAI. However, GPP simulated by the TL-LUE model exhibited a lower sensitivity to errors in PAR input data than the MOD17 model, indicating its robustness for simulating regional and global GPP using radiation data sets with large uncertainties.

Appendix A

Table A1 described the area proportions of different land cover types calculated from the Global Land Cover Data Set for each site over the central 1 km × 1 km or 3 km × 3 km around the flux tower. Area proportions of dominant vegetation types were highlighted in the table. Sites in this table were used to calibrate and validate TL-LUE and MOD17 models in this study.

Table A1. Area Proportions of Different Land Cover Types Calculated From the Global Land Cover Data Set for 98 Sites Over the Central 1 km × 1 km (for Crop, Grass, Savannas, Open Shrub, and Woody Savannas) or 3 km × 3 km (for Forests) Around the Tower[a]

				Area Proportion of GlobeLand30 Data Sets									
Site Name	Latitude (°)	Longitude (°)	LaThuile FLUXNET Vegetation Type	Crop	Forest	Grass	Shrub	Wetland	Water	Tundra	Artificial Surfaces	Bare Land	Snow and Ice
BE-Lon	50.55	4.74	Crop	**0.90**	0.00	0.00	0.00	0.00	0.00	0.00	0.10	0.00	0.00
CH-Oe2	47.29	7.73	Crop	**0.83**	0.02	0.00	0.00	0.00	0.00	0.00	0.14	0.00	0.00
CN-Yuc	36.95	116.60	Crop	**0.76**	0.00	0.00	0.00	0.00	0.00	0.00	0.24	0.00	0.00
DE-Geb	51.10	10.91	Crop	**1.00**	0.00	0.00	0.00	0.00	0.00	0.00	0.00	0.00	0.00
DE-Kli	50.89	13.52	Crop	**0.84**	0.07	0.00	0.00	0.00	0.00	0.00	0.08	0.00	0.00
DK-Ris	55.53	12.10	Crop	**0.98**	0.00	0.00	0.00	0.00	0.00	0.00	0.02	0.00	0.00
ES-ES2	39.28	−0.32	Crop	**1.00**	0.00	0.00	0.00	0.00	0.00	0.00	0.00	0.00	0.00
FR-Gri	48.84	1.95	Crop	**0.92**	0.01	0.00	0.00	0.00	0.00	0.00	0.07	0.00	0.00
IT-PT1	45.20	9.06	Crop	**0.51**	0.45	0.00	0.00	0.00	0.04	0.00	0.00	0.00	0.00
US-Bo1	40.01	−88.29	Crop	**1.00**	0.00	0.00	0.00	0.00	0.00	0.00	0.00	0.00	0.00
US-Bo2	40.01	−88.29	Crop	**1.00**	0.00	0.00	0.00	0.00	0.00	0.00	0.00	0.00	0.00
US-Ne1	41.17	−96.48	Crop	**0.98**	0.00	0.02	0.00	0.00	0.00	0.00	0.00	0.00	0.00
US-Ne2	41.16	−96.47	Crop	**0.99**	0.00	0.00	0.00	0.00	0.00	0.00	0.00	0.00	0.00
US-Ne3	41.18	−96.44	Crop	**0.95**	0.00	0.05	0.00	0.00	0.00	0.00	0.00	0.00	0.00
DE-Hai	51.08	10.45	DBF	0.17	**0.76**	0.06	0.00	0.00	0.00	0.00	0.00	0.00	0.00
FR-Fon	48.48	2.78	DBF	0.42	**0.45**	0.00	0.00	0.00	0.03	0.00	0.10	0.00	0.00

Table A1. (continued)

Site Name	Latitude (°)	Longitude (°)	LaThuile FLUXNET Vegetation Type	Area Proportion of GlobeLand30 Data Sets									
				Crop	Forest	Grass	Shrub	Wetland	Water	Tundra	Artificial Surfaces	Bare Land	Snow and Ice
FR-Hes	48.67	7.07	DBF	0.57	**0.37**	0.00	0.00	0.00	0.00	0.00	0.06	0.00	0.00
JP-Tak	36.15	137.42	DBF	0.04	**0.84**	0.11	0.00	0.00	0.00	0.00	0.00	0.01	0.00
US-Bar	44.06	−71.29	DBF	0.00	**0.92**	0.03	0.00	0.00	0.00	0.00	0.02	0.02	0.00
US-Ha1	42.54	−72.17	DBF	0.03	**0.95**	0.01	0.00	0.01	0.00	0.00	0.00	0.00	0.00
US-MMS	39.32	−86.41	DBF	0.02	**0.98**	0.00	0.00	0.00	0.00	0.00	0.00	0.00	0.00
US-MOz	38.74	−92.20	DBF	0.19	**0.75**	0.04	0.00	0.01	0.00	0.00	0.00	0.00	0.00
US-UMB	45.56	−84.71	DBF	0.02	**0.50**	0.12	0.00	0.13	0.24	0.00	0.00	0.00	0.00
US-WCr	45.81	−90.08	DBF	0.00	**0.83**	0.01	0.00	0.16	0.00	0.00	0.00	0.00	0.00
AU-Tum	−35.66	148.15	EBF	0.00	**1.00**	0.00	0.00	0.00	0.00	0.00	0.00	0.00	0.00
CN-Din	23.17	112.53	EBF	0.10	**0.73**	0.03	0.00	0.00	0.05	0.00	0.08	0.00	0.00
FR-Pue	43.74	3.60	EBF	0.02	**0.93**	0.03	0.00	0.00	0.00	0.00	0.00	0.02	0.00
GF-Guy	5.28	−52.91	EBF	0.00	**0.98**	0.01	0.00	0.00	0.00	0.00	0.01	0.00	0.00
ID-Pag	−2.35	114.04	EBF	0.00	**0.93**	0.06	0.00	0.00	0.00	0.00	0.00	0.00	0.00
IT-Cpz	41.71	12.38	EBF	0.08	**0.92**	0.00	0.00	0.00	0.00	0.00	0.00	0.00	0.00
CA-Ca1	49.87	−125.33	ENF	0.00	**0.93**	0.07	0.00	0.00	0.00	0.00	0.00	0.00	0.00
CA-Ca2	49.87	−125.29	ENF	0.00	**0.91**	0.06	0.00	0.01	0.00	0.00	0.01	0.01	0.00
CA-Ca3	49.53	−124.90	ENF	0.00	**0.78**	0.22	0.00	0.00	0.00	0.00	0.00	0.00	0.00
CA-Man	55.88	−98.48	ENF	0.00	**0.77**	0.02	0.00	0.21	0.01	0.00	0.00	0.00	0.00
CA-NS5	55.86	−98.49	ENF	0.00	**0.86**	0.03	0.00	0.09	0.01	0.00	0.00	0.00	0.00
CA-Qcu	49.27	−74.04	ENF	0.00	**0.94**	0.00	0.00	0.00	0.06	0.00	0.00	0.01	0.00
CA-Qfo	49.69	−74.34	ENF	0.00	**0.90**	0.00	0.00	0.04	0.04	0.00	0.00	0.01	0.00
CA-SJ2	53.94	−104.65	ENF	0.00	**0.77**	0.06	0.00	0.10	0.01	0.00	0.01	0.05	0.00
CA-SJ3	53.88	−104.65	ENF	0.00	**0.83**	0.05	0.00	0.08	0.00	0.00	0.03	0.02	0.00
CN-Qia	26.73	115.07	ENF	0.23	**0.75**	0.01	0.00	0.00	0.00	0.00	0.00	0.00	0.00
CZ-BK1	49.50	18.54	ENF	0.14	**0.86**	0.00	0.00	0.00	0.00	0.00	0.00	0.00	0.00
DE-Tha	50.96	13.57	ENF	0.38	**0.56**	0.00	0.00	0.00	0.00	0.00	0.06	0.00	0.00
DE-Wet	50.45	11.46	ENF	0.22	**0.74**	0.00	0.00	0.00	0.00	0.00	0.04	0.00	0.00
FI-Hyy	61.85	24.29	ENF	0.06	**0.91**	0.00	0.00	0.00	0.03	0.00	0.00	0.00	0.00
IL-Yat	31.35	35.05	ENF	0.00	**0.50**	0.50	0.00	0.00	0.00	0.00	0.00	0.00	0.00
IT-Bon	39.48	16.53	ENF	0.23	**0.73**	0.01	0.00	0.00	0.00	0.00	0.00	0.03	0.00
IT-Ren	46.59	11.43	ENF	0.14	**0.85**	0.00	0.00	0.00	0.00	0.00	0.00	0.00	0.00
NL-Loo	52.17	5.74	ENF	0.20	**0.71**	0.00	0.00	0.00	0.00	0.00	0.01	0.07	0.00
PT-Esp	38.64	−8.60	ENF	0.24	**0.74**	0.00	0.00	0.00	0.01	0.00	0.02	0.00	0.00
RU-Fyo	56.46	32.92	ENF	0.08	**0.88**	0.02	0.00	0.00	0.00	0.00	0.02	0.00	0.00
SE-Fla	64.11	19.46	ENF	0.06	**0.89**	0.00	0.00	0.04	0.01	0.00	0.00	0.00	0.00
SE-Nor	60.09	17.48	ENF	0.09	**0.85**	0.00	0.00	0.03	0.03	0.00	0.00	0.00	0.00
SE-Sk1	60.13	17.92	ENF	0.06	**0.89**	0.00	0.00	0.04	0.01	0.00	0.00	0.00	0.00
US-Blo	38.90	−120.63	ENF	0.00	**0.91**	0.07	0.00	0.00	0.01	0.00	0.00	0.00	0.00
US-Ho1	45.20	−68.74	ENF	0.00	**0.97**	0.02	0.00	0.00	0.00	0.00	0.00	0.00	0.00
US-Me2	44.45	−121.56	ENF	0.00	**1.00**	0.00	0.00	0.00	0.00	0.00	0.00	0.00	0.00
US-Me3	44.32	−121.61	ENF	0.01	**0.98**	0.00	0.00	0.00	0.00	0.00	0.00	0.00	0.00
US-NC2	35.80	−76.67	ENF	0.29	**0.65**	0.06	0.00	0.00	0.00	0.00	0.00	0.00	0.00
US-NR1	40.03	−105.55	ENF	0.00	**0.96**	0.03	0.00	0.00	0.00	0.00	0.00	0.00	0.00
US-SP1	29.74	−82.22	ENF	0.02	**0.80**	0.01	0.00	0.16	0.00	0.00	0.02	0.00	0.00
US-SP2	29.76	−82.24	ENF	0.08	**0.63**	0.02	0.00	0.24	0.00	0.00	0.01	0.01	0.00
US-SP3	29.75	−82.16	ENF	0.01	**0.76**	0.01	0.00	0.15	0.04	0.00	0.03	0.00	0.00
CA-Let	49.71	−112.94	Grass	0.43	0.00	**0.56**	0.00	0.00	0.00	0.00	0.00	0.00	0.00
CH-Oe1	47.29	7.73	Grass	0.00	0.01	**0.80**	0.00	0.00	0.00	0.00	0.19	0.00	0.00
CN-Ha2	37.67	101.33	Grass	0.00	0.00	**1.00**	0.00	0.00	0.00	0.00	0.00	0.00	0.00
DE-Meh	51.28	10.66	Grass	0.00	0.02	**0.96**	0.00	0.00	0.00	0.00	0.02	0.00	0.00
FR-Lq1	45.64	2.74	Grass	0.00	0.00	**0.96**	0.02	0.00	0.00	0.00	0.01	0.00	0.00
FR-Lq2	45.64	2.74	Grass	0.00	0.00	**0.96**	0.02	0.00	0.00	0.00	0.01	0.00	0.00
HU-Bug	46.69	19.60	Grass	0.00	0.24	**0.72**	0.04	0.00	0.00	0.00	0.00	0.00	0.00
IE-Dri	51.99	−8.75	Grass	0.00	0.00	**0.99**	0.00	0.00	0.00	0.00	0.01	0.00	0.00
IT-MBo	46.03	11.08	Grass	0.00	0.92	**0.92**	0.01	0.00	0.00	0.00	0.00	0.07	0.00
SE-Deg	64.18	19.56	Grass	0.00	0.08	**0.92**	0.00	0.00	0.00	0.00	0.00	0.00	0.00
US-Wkg	31.74	−109.94	Grass	0.00	0.00	**0.98**	0.00	0.00	0.00	0.00	0.02	0.00	0.00
US-FPe	48.31	−105.10	Grass	0.19	0.00	**0.71**	0.05	0.03	0.00	0.00	0.00	0.01	0.00

Table A1. (continued)

Site Name	Latitude (°)	Longitude (°)	LaThuile FLUXNET Vegetation Type	Area Proportion of GlobeLand30 Data Sets									
				Crop	Forest	Grass	Shrub	Wetland	Water	Tundra	Artificial Surfaces	Bare Land	Snow and Ice
BE-Bra	51.31	4.52	MF	0.17	**0.34**	0.00	0.00	0.00	0.01	0.00	0.47	0.00	0.00
BE-Vie	50.31	6.00	MF	0.13	**0.58**	0.00	0.00	0.00	0.00	0.00	0.30	0.00	0.00
CA-Gro	48.22	−82.16	MF	0.00	**0.91**	0.05	0.00	0.00	0.03	0.00	0.01	0.00	0.00
CA-Oas	53.63	−106.20	MF	0.00	**0.95**	0.00	0.00	0.01	0.04	0.00	0.00	0.00	0.00
CA-Obs	53.99	−105.12	MF	0.00	**0.80**	0.01	0.00	0.16	0.00	0.00	0.02	0.01	0.00
CA-TP4	42.71	−80.36	MF	0.41	**0.46**	0.05	0.00	0.02	0.03	0.00	0.01	0.00	0.00
CA-WP1	54.95	−112.47	MF	0.07	**0.86**	0.04	0.00	0.00	0.00	0.00	0.03	0.00	0.00
CN-Cha	42.40	128.10	MF	0.03	**0.83**	0.04	0.00	0.00	0.00	0.00	0.10	0.00	0.00
DE-Gri	50.95	13.51	MF	0.16	**0.82**	0.00	0.00	0.00	0.00	0.00	0.02	0.00	0.00
DE-Har	47.93	7.60	MF	0.55	**0.31**	0.00	0.00	0.00	0.07	0.00	0.07	0.00	0.00
IT-Lav	45.96	11.28	MF	0.13	**0.83**	0.00	0.00	0.00	0.00	0.00	0.02	0.01	0.00
US-Dk1	35.97	−79.09	MF	0.08	**0.82**	0.01	0.00	0.02	0.00	0.00	0.05	0.00	0.00
US-Dk2	35.97	−79.10	MF	0.10	**0.83**	0.01	0.00	0.02	0.00	0.00	0.03	0.00	0.00
US-Dk3	35.98	−79.09	MF	0.10	**0.83**	0.01	0.00	0.02	0.00	0.00	0.03	0.00	0.00
US-PFa	45.95	−90.27	MF	0.01	**0.62**	0.04	0.00	0.33	0.01	0.00	0.00	0.00	0.00
US-Syv	46.24	−89.35	MF	0.00	**0.70**	0.01	0.00	0.15	0.13	0.00	0.00	0.00	0.00
CA-NS6	55.92	−98.96	OS	0.00	0.03	0.01	**0.93**	0.00	0.02	0.00	0.00	0.00	0.00
CA-NS7	56.64	−99.95	OS	0.00	0.10	0.00	**0.68**	0.09	0.10	0.00	0.03	0.00	0.00
US-Aud	31.59	−110.51	OS	0.00	0.00	0.00	**1.00**	0.00	0.00	0.00	0.00	0.00	0.00
US-SRM	31.82	−110.87	OS	0.00	0.07	0.00	**0.93**	0.00	0.00	0.00	0.00	0.00	0.00
AU-How	−12.49	131.15	Savannas	0.00	**0.50**	0.44	0.01	0.06	0.00	0.00	0.00	0.00	0.00
ES-VDA	42.15	1.45	Savannas	0.00	0.45	0.00	**0.55**	0.00	0.00	0.00	0.00	0.00	0.00
US-KS2	28.61	−80.67	WS	0.02	0.06	0.00	0.00	**0.62**	0.21	0.00	0.10	0.00	0.00
US-Ton	38.43	−120.97	WS	0.00	0.00	**0.60**	0.40	0.00	0.00	0.00	0.00	0.00	0.00

[a]The highlighted table entries mean the area proportions of dominant vegetation types.

Table A2 described site years used for calibrating and validating TL-LUE and MOD17 models, as well as the basic characteristics of each site, including abbreviated name, country, latitude, longitude, vegetation types, and related references.

Table A2. Characteristics of the FLUXNET Sites Used in This Study[a]

Site Name	Country	Latitude (°)	Longitude (°)	LaThuile FLUXNET Vegetation Type	Calibration Years	Validation Years	Reference
BE-Lon	Belgium	50.55	4.74	Crop		2004	*Stoy et al.* [2013]
CH-Oe2	Switzerland	47.29	7.73	Crop		2005	*Eugstera et al.* [2010]
CN-Yuc	China	36.95	116.60	Crop		2003-2004	*Yu et al.* [2006]
DE-Geb	Germany	51.10	10.91	Crop	2005	2004	*Kutsch et al.* [2010]
DE-Kli	Germany	50.89	13.52	Crop	2005		*Wattenbach et al.* [2010]
DK-Ris	Denmark	55.53	12.10	Crop	2004-2005		*Eugstera et al.* [2010]
ES-ES2	Spain	39.28	-0.32	Crop	2005		*Stoy et al.* [2013]
FR-Gri	France	48.84	1.95	Crop		2005	*Stoy et al.* [2013]
IT-PT1	Italy	45.20	9.06	Crop	2003		*Stoy et al.* [2013]
US-Bo1	US	40.01	-88.29	Crop	2002-2003	2004	*Blyth et al.* [2011]
US-Bo2	US	40.01	-88.29	Crop		2004	*Reichstein et al.* [2005]
US-Ne1	US	41.17	-96.48	Crop	2002-2004		*Ershadi et al.* [2014]
US-Ne2	US	41.16	-96.47	Crop	2003-2004		*Ershadi et al.* [2014]
US-Ne3	US	41.18	-96.44	Crop	2003-2004	2001	*Ershadi et al.* [2014]
DE-Hai	Germany	51.08	10.45	DBF	2001,2003-2005	2002	*Knohl et al.* [2003]
FR-Fon	France	48.48	2.78	DBF		2006	*Smith et al.* [2010]
FR-Hes	France	48.67	7.07	DBF	2001-2005	2006	*Stoy et al.* [2013]
JP-Tak	Japan	36.15	137.42	DBF		2001-2004	*Kume et al.* [2011]
US-Bar	US	44.06	-71.29	DBF	2004	2005	*Jenkins et al.* [2007]

Table A2. (continued)

Site Name	Country	Latitude (°)	Longitude (°)	LaThuile FLUXNET Vegetation Type	Calibration Years	Validation Years	Reference
US-Ha1	US	42.54	-72.17	DBF	2000-2001,2006	2004	*Blyth et al.* [2011]
US-MMS	US	39.32	-86.41	DBF	2001, 2003, 2005	2002	*Schmid et al.* [2000]
US-MOz	US	38.74	-92.20	DBF	2005	2006	*Gu et al.* [2006]
US-UMB	US	45.56	-84.71	DBF	2001-2003		*Gough et al.* [2013]
US-WCr	US	45.81	-90.08	DBF	2002, 2005	2003	*Cook et al.* [2004]
AU-Tum	Austria	-35.66	148.15	EBF	2003-2005	2002	*Lasslop et al.* [2010]
CN-Din	China	23.17	112.53	EBF	2003-2004	2005-2006	*Yu et al.* [2006]
FR-Pue	France	43.74	3.60	EBF	2001,2003-2005	2002	*Stoy et al.* [2013]
GF-Guy	French Guiana	5.28	-52.91	EBF	2004-2005		*Bonal et al.* [2008]
ID-Pag	Indonesia	-2.35	114.04	EBF	2002		*Hirata et al.* [2008]
IT-Cpz	Italy	41.71	12.38	EBF		2002	*Garbulksy et al.* [2008]
CA-Ca1	Canada	49.87	-125.33	ENF	2001, 2003-2005	2002	*Humphreys et al.* [2006]
CA-Ca2	Canada	49.87	-125.29	ENF	2001-2004	2005	*Humphreys et al.* [2006]
CA-Ca3	Canada	49.53	-124.90	ENF	2002-2004	2005	*Humphreys et al.* [2006]
CA-Man	Canada	55.88	-98.48	ENF	2003	2001	*Hilton et al.* [2014]
CA-NS5	Canada	55.86	-98.49	ENF	2004		*Goulden et al.* [2006]
CA-Qcu	Canada	49.27	-74.04	ENF	2002-2003, 2005	2004	*Giasson et al.* [2006]
CA-Qfo	Canada	49.69	-74.34	ENF	2005	2004	*Bergeron et al.* [2007]
CA-SJ2	Canada	53.94	-104.65	ENF	2004-2005		*Zha et al.* [2009]
CA-SJ3	Canada	53.88	-104.65	ENF	2005		*Zha et al.* [2009]
CN-Qia	China	26.73	115.07	ENF	2003-2004	2005-2006	*Yu et al.* [2006]
CZ-BK1	Czech	49.50	18.54	ENF	2004-2006		*Smith et al.* [2010]
DE-Tha	Germany	50.96	13.57	ENF	2001-2005		*Grünwald and Berhofer* [2007]
DE-Wet	Germany	50.45	11.46	ENF	2003-2005		*Rebmann et al.* [2010]
FI-Hyy	Finland	61.85	24.29	ENF	2001-2004		*Suni et al.* [2003]
IL-Yat	Israel	31.35	35.05	ENF		2001-2002	*Sprintsin et al.* [2011]
IT-Bon	Italy	39.48	16.53	ENF		2006	*Smith et al.* [2010]
IT-Ren	Italy	46.59	11.43	ENF		2001-2003	*Montagnani et al.* [2009]
NL-Loo	Netherlands	52.17	5.74	ENF	2001-2005		*Dolman et al.* [2002]
PT-Esp	Portugal	38.64	-8.60	ENF	2003-2004		*Wei et al.* [2014]
RU-Fyo	Russia	56.46	32.92	ENF		2001-2006	*Milyukova et al.* [2002]
SE-Fla	Sweden	64.11	19.46	ENF	2001-2002		*Smith et al.* [2010]
SE-Nor	Sweden	60.09	17.48	ENF	2003		*Lagergren et al.* [2008]
SE-Sk1	Sweden	60.13	17.92	ENF	2005		*Stoy et al.* [2013]
US-Blo	US	38.90	-120.63	ENF	2001-2003, 2005		*Goldstein et al.* [2000]
US-Ho1	US	45.20	-68.74	ENF		2000-2004	*Stoy et al.* [2013]
US-Me2	US	44.45	-121.56	ENF	2005		*Stoy et al.* [2013]
US-Me3	US	44.32	-121.61	ENF	2004-2005		*Vickers et al.* [2009]
US-NC2	US	35.80	-76.67	ENF	2005	2006	*Noormets et al.* [2010]
US-NR1	US	40.03	-105.55	ENF	2000, 2002-2003		*Monson et al.* [2002]
US-SP1	US	29.74	-82.22	ENF	2005		*Stoy et al.* [2013]
US-SP2	US	29.76	-82.24	ENF	2000-2001, 2003-2004		*Glenn et al.* [2010]
US-SP3	US	29.75	-82.16	ENF	2001-2004		*Hilton et al.* [2014]
CA-Let	Canada	49.71	-112.94	Grass	2002-2005	2001	*Flanagan and Adkinson* [2011]
CH-Oe1	Switzerland	47.29	7.73	Grass		2003	*Ammann et al.* [2007]
CN-Ha2	China	37.67	101.33	Grass		2005-2006	*Zhang et al.* [2008]
DE-Meh	Germany	51.28	10.66	Grass	2004-2006		*Stoy et al.* [2013]
FR-Lq1	France	45.64	2.74	Grass	2004-2006		*Gilmanov et al.* [2007]
FR-Lq2	France	45.64	2.74	Grass	2004-2006		*Gilmanov et al.* [2007]
HU-Bug	Hungary	46.69	19.60	Grass	2003-2006		*Stoy et al.* [2013]
IE-Dri	Ireland	51.99	-8.75	Grass	2004	2003	*Stoy et al.* [2013]
IT-MBo	Italy	46.03	11.08	Grass		2003-2006	*Gianelle et al.* [2009]
SE-Deg	Sweden	64.182	19.557	Grass	2001-2002, 2004-2005		*Smith et al.* [2010]
US-FPe	US	48.31	-105.10	Grass	2003-2004		*Ershadi et al.* [2014]
US-Wkg	US	31.74	-109.94	Grass	2006		*Scott* [2010]
BE-Bra	Belgium	51.31	4.52	MF	2002, 2004		*Stoy et al.* [2013]
BE-Vie	Belgium	50.31	6.00	MF	2001-2005		*Aubinet et al.* [2001]
CA-Gro	Canada	48.22	-82.16	MF	2004		*McCaughey et al.* [2006]
CA-Oas	Canada	53.63	-106.20	MF	2000, 2002-2005	2001	*Black et al.* [2000]
CA-Obs	Canada	53.99	-105.12	MF	2000-2003, 2005	2004	*Krishnan et al.* [2008]

Table A2. (continued)

Site Name	Country	Latitude (°)	Longitude (°)	LaThuile FLUXNET Vegetation Type	Calibration Years	Validation Years	Reference
CA-TP4	Canada	42.71	-80.36	MF	2005	2004	*Arain and Restrepo-Coupe* [2005]
CA-WP1	Canada	54.95	-112.47	MF	2004-2005		*Flanagan and Syed* [2011]
CN-Cha	China	42.40	128.10	MF	2005-2006	2003-2004	*Yu et al.* [2006]
DE-Gri	Germany	50.95	13.51	MF	2005-2006		*Smith et al.* [2010]
DE-Har	Germany	47.93	7.60	MF	2005-2006		*Stoy et al.* [2013]
IT-Lav	Italy	45.96	11.28	MF	2001-2002		*Marcolla et al.* [2003]
US-Dk1	US	35.97	-79.09	MF	2003-2004		*Gilmanov et al.* [2010]
US-Dk2	US	35.97	-79.10	MF	2003-2005		*Pataki and Oren* [2003]
US-Dk3	US	35.98	-79.09	MF	2002-2004		*Pataki and Oren* [2003]
US-PFa	US	45.95	-90.27	MF		2003	*Davis et al.* [2003]
US-Syv	US	46.24	-89.35	MF		2002	*Desai et al.* [2005]
CA-NS6	Canada	55.92	-98.96	OS	2002, 2004	2003	*Goulden et al.* [2006]
CA-NS7	Canada	56.64	-99.95	OS	2004	2003	*Goulden et al.* [2011]
US-Aud	US	31.59	-110.51	OS	2005		*Horn and Schulz* [2011]
US-SRM	US	31.82	-110.87	OS	2004-2006		*Scott* [2010]
AU-How	Austria	-12.49	131.15	Savannas	2002, 2005		*Ershadi et al.* [2014]
ES-VDA	Spain	42.15	1.45	Savannas	2005	2004	*Gilmanov et al.* [2007]
US-KS2	US	28.61	-80.67	WS	2004-2005	2002	*Powell et al.* [2006]
US-Ton	US	38.43	-120.97	WS	2002-2003, 2005-2006	2004	*Hilton et al.* [2014]

[a]The site name codes are a composition of country (first two letters) and site name (last three letters). Investigator-provided vegetation types are deciduous broadleaf forest (DBF), evergreen broadleaf forest (EBF), evergreen needleleaf forest (ENF), mixed forest (MF), Crop (crop), Grass(grass), open shrub (OS), savanna (Savannas) and woody savanna (WS).

Table A3 described the basic characteristics of the flux sites used for validating direct and diffuse radiation calculated in this study in Figure 1, including abbreviated name, country, latitude, longitude, vegetation types, and related references.

Table A3. Characteristics of the FLUXNET Sites Used for Validating Direct and Diffuse Radiation[a]

Site	Country	Latitude (°)	Longitude (°)	LaThuile FLUXNET Vegetation Type	Years	References
CH-Oe2	Switzerland	47.29	7.73	Crop	2005	*Eugstera et al.* [2010]
US-Ne1	US	41.17	-96.48	Crop	2002-2004	*Ershadi et al.* [2014]
US-Ne2	US	41.16	-96.47	Crop	2002-2004	*Ershadi et al.* [2014]
US-Ne3	US	41.18	-96.44	Crop	2002-2004	*Ershadi et al.* [2014]
FR-Fon	France	48.48	2.78	DBF	2006	*Smith et al.* [2010]
FR-Hes	France	48.67	7.07	DBF	2006	*Stoy et al.* [2013]
IT-Ro1	Italy	42.41	11.93	DBF	2006	*Wei et al.* [2014]
US-Bar	US	44.06	-71.29	DBF	2005	*Jenkins et al.* [2007]
FR-Pue	France	43.74	3.60	EBF	2005-2006	*Stoy et al.* [2013]
VU-Coc	Vanuatu	-15.44	167.19	EBF	2002-2003	*Roupsard et al.* [2006]
DE-Wet	Germany	50.45	11.46	ENF	2005-2006	*Rebmann et al.* [2010]
FI-Hyy	Finland	61.85	24.29	ENF	2004-2005	*Suni et al.* [2003]
FR-LBr	France	44.72	-0.77	ENF	2003-2005	*Stoy et al.* [2013]
IT-SRo	Italy	43.73	10.28	ENF	2006	*Wei et al.* [2014]
NL-Loo	Netherlands	52.17	5.74	ENF	2005-2006	*Dolman et al.* [2002]
DE-Meh	Germany	51.28	10.66	Grass	2004, 2006	*Stoy et al.* [2013]
IT-Amp	Italy	41.90	13.61	Grass	2006	*Gilmanov et al.* [2007]
IT-Mbo	Italy	46.03	11.08	Grass	2005-2006	*Gianelle et al.* [2009]
NL-Ca1	Netherlands	51.971	4.927	Grass	2006	*Stoy et al.* [2013]
US-Var	US	38.41	-120.95	Grass	2006	*Stoy et al.* [2013]
IT-Lav	Italy	45.96	11.28	MF	2006	*Marcolla et al.* [2003]
ES-LMa	Spain	39.94	-5.77	Savannas	2004	*Stoy et al.* [2013]

[a]The site name codes are a composition of country (first two letters) and site name (last three letters). Investigator-provided vegetation types are deciduous broadleaf forest (DBF), evergreen broadleaf forest (EBF), evergreen needleleaf forest (ENF), mixed forest (MF), Crop (crop), Grass(grass), and savanna (Savannas).

Acknowledgments
This work was supported by National Natural Science Foundation of China (41371070), Special climate change fund (CCSF201412), and Chinese Academy of Sciences (XDA05050602-1). This research is based in part on support from the Department of Energy's (DOE) National Institute for Climate Change Research (NICCR) (07-SC-NICCR-1059), the National Science Foundation(NSF) Division of Atmospheric and Geospace Sciences (AGS), Atmospheric Chemistry program (1233006), NSF award EF1137306/MIT subaward 5710003122 to the University of California, Davis and NSF through the Florida Coastal Everglades Long Term Ecological Research program (DBI-0620409 and DEB-9910514). The data for this paper are available at FLUXNET data set (http://www.fluxdata.org/DataInfo). Data set: LaThuile. The data acquired by the FLUXNET community as part of the La Thuile collection and in particular by the following networks: AmeriFlux (U.S. Department of Energy, Biological and Environmental Research, Terrestrial Carbon Program (DE-FG02-04ER63917 and DE-FG02-04ER63911)), AfriFlux, AsiaFlux, CarboAfrica, CarboEuropeIP, Carboltaly, CarboMont, ChinaFlux, Fluxnet-Canada (supported by CFCAS, NSERC, BIOCAP, Environment Canada, and NRCan), GreenGrass, KoFlux, LBA, NECC, OzFlux, TCOS-Siberia, and USCCC. We appreciate the financial support to the eddy covariance data harmonization provided by CarboEuropeIP, FAO-GTOS-TCO, iLEAPS, Max Planck Institute for Biogeochemistry, National Science Foundation, University of Tuscia, Université Laval and Environment Canada, and U.S. Department of Energy and the database development and technical support from Bekeley Water Center, Lawrence Berkeley National Laboratory, Microsoft Research eScience, Oak Ridge National Laboratory, University of California-Berkeley, University of Virginia.

References

Akaike, H. (1974), A new look at the statistical model identification, *IEEE Trans. Autom. Control*, *19*(6), 716–723, doi:10.1109/TAC.1974.1100705.

Alton, P. B. (2008), Reduced carbon sequestration in terrestrial ecosystems under overcast skies compared to clear skies, *Agric. For. Meteorol.*, *148*(10), 1641–1653, doi:10.1016/j.agrformet.2008.05.014.

Alton, P. B., P. R. North, and S. O. Los (2007), The impact of diffuse sunlight on canopy light-use efficiency, gross photosynthetic product and net ecosystem exchange in three forest biomes, *Global Change Biol.*, *13*(4), 776–787, doi:10.1111/j.1365-2486.2007.01316.x.

Ammann, C., C. R. Flechard, J. Leifeld, A. Neftel, and J. Fuhrer (2007), The carbon budget of newly established temperate grassland depends on management intensity, Agriculture, *Ecosyst. Environ.*, *121*(1–2), 5–20, doi:10.1016/j.agee.2006.12.002.

Arain, M. A., and N. Restrepo-Coupe (2005), Net ecosystem production in a temperate pine plantation in southeastern Canada, *Agric. For. Meteorol.*, *128*(3–4), 223–241, doi:10.1016/j.agrformet.2004.10.003.

Aubinet, M., B. Chermanne, M. Vandenhaute, B. Longdoz, M. Yernaux, and E. Laitat (2001), Long term carbon dioxide exchange above a mixed forest in the Belgian Ardennes, *Agric. For. Meteorol.*, *108*(4), 293–315, doi:10.1016/S0168-1923(01)00244-1.

Baldocchi, D. (1997), Measuring and modelling carbon dioxide and water vapour exchange over a temperate broad-leaved forest during the 1995 summer drought, *Plant Cell Environ.*, *20*(9), 1108–1122, doi:10.1046/j.1365-3040.1997.d01-147.x.

Baldocchi, D. (2008), Turner Review No. 15. 'Breathing' of the terrestrial biosphere: Lessons learned from a global network of carbon dioxide flux measurement systems, *Aust. J. Bot.*, *56*, 1–26, doi:10.1071/BT07151.

Baldocchi, D. (2014), Measuring fluxes of trace gases and energy between ecosystems and the atmosphere—The state and future of the eddy covariance method, *Global Change Biol.*, *20*(12), 3600–3609, doi:10.1111/gcb.12649.

Baldocchi, D., et al. (2001), FLUXNET: A new tool to study the temporal and spatial variability of ecosystem-scale carbon dioxide, water vapor, and energy flux densities, *Bull. Am. Meteorol. Soc.*, *82*(11), 2415–2434, doi:10.1175/1520-0477(2001)082<2415:FANTTS>2.3.CO;2.

Baldocchi, D. D. (2003), Assessing the eddy covariance technique for evaluating carbon dioxide exchange rates of ecosystems: Past, present and future, *Global Change Biol.*, *9*(4), 479–492, doi:10.1046/j.1365-2486.2003.00629.x.

Baldocchi, D. D., et al. (2005), Predicting the onset of net carbon uptake by deciduous forests with soil temperature and climate data: A synthesis of FLUXNET data, *Int. J. Biometeorol.*, *49*(6), 377–387, doi:10.1007/s00484-005-0256-4.

Beer, C., et al. (2010), Terrestrial gross carbon dioxide uptake: Global distribution and covariation with climate, *Science*, *329*, 834–838, doi:10.1126/science.1184984.

Bergeron, O., H. A. Margolis, T. A. Black, C. Coursolle, A. L. Dunn, A. G. Barr, and S. C. Wofsy (2007), Comparison of carbon dioxide fluxes over three boreal black spruce forests in Canada, *Global Change Biol.*, *13*(1), 89–107, doi:10.1111/j.1365-2486.2006.01281.x.

Betts, A. K., S. Y. Hong, and H. L. Pan (1996), Comparison of NCEP-NCAR reanalysis with 1987 FIFE data, *Mon. Weather Rev.*, *124*(7), 1480–1498, doi:10.1175/1520-0493(1996)124<1480:CONNRW>2.0.CO;2.

Black, T. A., W. J. Chen, and A. G. Barr (2000), Increased carbon sequestration by a boreal deciduous forest in years with a warm spring, *Geophys. Res. Lett.*, *27*(9), 1271–1274, doi:10.1029/1999GL011234.

Blyth, E., D. B. Clark, R. Ellis, C. Huntingford, S. Los, M. Pryor, M. Best, and S. Sitch (2011), A comprehensive set of benchmark tests for a land surface model of simultaneous fluxes of water and carbon at both the global and seasonal scale, *Geosci. Model Dev.*, *4*(2), 255–269, doi:10.5194/gmd-4-255-2011.

Bonal, D., et al. (2008), Impact of severe dry season on net ecosystem exchange in the Neotropical rainforest of French Guiana, *Global Change Biol.*, *14*(8), 1917–1933, doi:10.1111/j.1365-2486.2008.01610.x.

Bosch, J. L., G. López, and F. J. Batlles (2009), Global and direct photosynthetically active radiation parameterizations for clear-sky conditions, *Agric. For. Meteorol.*, *149*(1), 146–158, doi:10.1016/j.agrformet.2008.07.011.

Brotzge, J. A. (2004), A two-year comparison of the surface water and energy budgets between two OASIS sites and NCEP-NCAR reanalysis data, *J. Hydrometeorol.*, *5*(2), 311–326, doi:10.1175/1525-7541(2004)005<0311:ATCOTS>2.0.CO;2.

Brovelli, M. A., M. E. Molinari, E. Hussein, J. Chen, and R. Li (2015), The first comprehensive accuracy assessment of GlobeLand30 at a national level: Methodology and results, *Remote Sens.*, *7*(4), 4191–4212.

Cai, T., A. Black, R. S. Jassal, K. Morgenstern, and Z. Nesic (2009), Incorporating diffuse photosynthetically active radiation in a single-leaf model of canopy photosynthesis for a 56-year-old coastal Douglas-fir forest, *Int. J. Biometeorol.*, *53*(2), 135–148, doi:10.1007/s00484-008-0196-x.

Cao, X., J. Chen, L. Chen, A. Liao, F. Sun, Y. Li, L. Li, Z. Lin, Z. Pang, and J. Chen (2014), Preliminary analysis of spatiotemporal pattern of global land surface water, *Sci. China-Earth Sci.*, *57*(10), 2330–2339.

Chen, B. Z., et al. (2012), Characterizing spatial representativeness of flux tower eddy-covariance measurements across the Canadian Carbon Program Network using remote sensing and footprint analysis, *Remote Sens. Environ.*, *124*, 742–755, doi:10.1016/j.rse.2012.06.007.

Chen, J., J. Chen, A. Liao, X. Cao, L. Chen, X. Chen, C. He, G. Han, S. Peng, and M. Lu (2015), Global land cover mapping at 30 m resolution: A POK-based operational approach, *ISPRS J. Photogramm. Remote Sens.*, *103*, 7–27.

Chen, J. M., J. Liu, J. Cihlar, and M. L. Goulden (1999), Daily canopy photosynthesis model through temporal and spatial scaling for remote sensing applications, *Ecol. Modell.*, *124*(2–3), 99–119, doi:10.1016/S0304-3800(99)00156-8.

Chen, J. M., F. Deng, and M. Chen (2006), Locally adjusted cubic-spline capping for reconstructing seasonal trajectories of a satellite-derived surface parameter, *IEEE Trans. Geosci. Remote Sens.*, *44*(8), 2230–2238, doi:10.1109/TGRS.2006.872089.

Chen, T., G. R. van der Werf, A. J. Dolman, and M. Groenendijk (2011), Evaluation of cropland maximum light use efficiency using eddy flux measurements in North America and Europe, *Geophys. Res. Lett.*, *38*, L14707, doi:10.1029/2011GL047533.

Choudhury, B. J. (2001), Estimating gross photosynthesis using satellite and ancillary data: Approach and preliminary results, *Remote Sens. Environ.*, *75*(1), 1–21, doi:10.1016/S0034-4257(00)00151-6.

Cohan, D. S., J. Xu, R. Greenwald, M. H. Bergin, and W. L. Chameides (2002), Impact of atmospheric aerosol light scattering and absorption of terrestrial net primary productivity, *Global Biogeochem. Cycles*, *16*(4), 1090, doi:10.1029/2001GB001441.

Cook, B. D., et al. (2004), Carbon exchange and venting anomalies in an upland deciduous forest in northern Wisconsin, USA, *Agric. For. Meteorol.*, *126*(3–4), 271–295, doi:10.1016/j.agrformet.2004.06.008.

Davis, K. J., P. S. Bakwin, C. Yi, B. W. Berger, C. Zhao, R. Teclaw, and J. G. Isebrands (2003), The annual cycles of CO_2 and H_2O exchange over a northern mixed forest as observed from a very tall tower, *Global Change Biol.*, *9*(9), 1278–1293, doi:10.1046/j.1365-2486.2003.00672.x.

De Pury, D. G. G., and G. D. Farquhar (1997), Simple scaling of photosynthesis from leaves to canopies without the errors of big-leaf models, *Plant, Cell Environ.*, *20*(5), 537–557, doi:10.1111/j.1365-3040.1997.00094.x.

Desai, A. R., P. V. Bolstad, B. D. Cook, K. J. Davis, and E. V. Carey (2005), Comparing net ecosystem exchange of carbon dioxide between an old-growth and mature forest in the upper Midwest, USA, *Agric. For. Meteorol.*, *128*(1–2), 33–55, doi:10.1016/j.agrformet.2004.09.005.

Dolman, A. J., E. J. Moors, and J. A. Elbers (2002), The carbon uptake of amid latitude forest on sandy soil, *Agric. For. Meteorol.*, *111*(3), 157–170, doi:10.1016/S0168-1923(02)00024-2.

Duan, Q. Y., S. Sorooshian, and V. Gupta (1992), Effective and efficient global optimization for conceptual rain full-runoff models, *Water Resour. Res.*, *28*(4), 1015–1031, doi:10.1029/91WR02985.

Ershadi, A., M. F. McCabe, J. P. Evans, N. W. Chaney, and E. F. Wood (2014), Multi-site evaluation of terrestrial evaporation models using FLUXNET data, *Agric. For. Meteorol.*, *187*, 46–61, doi:10.1016/j.agrformet.2013.11.008.

Eugstera, W., et al. (2010), Management effects on European cropland respiration, *Agric. Ecosyst. Environ.*, *139*(3), 346–362, doi:10.1016/j.agee.2010.09.001.

Falge, E., et al. (2002), Seasonality of ecosystem respiration and gross primary production as derived from FLUXNET measurements, *Agric. For. Meteorol.*, *113*(1–4), 53–74, doi:10.1016/S0168-1923(02)00102-8.

Fang, H. L., S. S. Wei, C. Y. Jiang, and K. Scipal (2012), Theoretical uncertainty analysis of global MODIS, CYCLOPES, and GLOBCARBON LAI products using a triple collocation method, *Remote Sens. Environ.*, *124*, 610–621, doi:10.1016/j.rse.2012.06.013.

Flanagan, L. B., and A. C. Adkinson (2011), Interacting controls on productivity in a northern Great Plains grassland and implications for response to ENSO events, *Global Change Biol.*, *17*(11), 3293–3311, doi:10.1111/j.1365-2486.2011.02461.x.

Flanagan, L. B., and K. H. Syed (2011), Stimulation of both photosynthesis and respiration in response to warmer and drier conditions in a boreal peatland ecosystem, *Global Change Biol.*, *17*(7), 2271–2287, doi:10.1111/j.1365-2486.2010.02378.x.

Foley, J. A., I. C. Prentice, N. Ramankutty, S. Levis, D. Pollard, S. Sitch, and A. Haxeltine (1996), An integrated biosphere model of land surface processes, terrestrial carbon balance, and vegetation dynamics, *Global Biogeochem. Cycles*, *10*(4), 603–628, doi:10.1029/96GB02692.

Freedman, J. M., D. R. Fitzjarrald, K. E. Moore, and R. K. Sakai (2001), Boundary layer clouds and vegetation-atmosphere feedbacks, *J. Clim.*, *14*(2), 180–197, doi:10.1175/1520-0442(2001)013<0180:BLCAVA>2.0.CO;2.

Friend, A. D. (2001), Modelling canopy CO_2 fluxes: Are 'big-leaf' simplifications justified, *Global Ecol. Biogeogr.*, *10*(6), 603–619, doi:10.1046/j.1466-822x.2001.00268.x.

Garbulksy, M. F., J. Penuelas, D. Papale, and I. Fillela (2008), Remote estimation of carbon dioxide uptake by a Mediterranean forest, *Global Change Biol.*, *14*(12), 2860–2867, doi:10.1111/j.1365-2486.2008.01684.x.

Garbulsky, M. F., J. Peñuelas, D. Papale, J. Ardö, M. L. Goulden, G. Kiely, A. D. Richardson, E. Rotenberg, E. M. Veenendaal, and I. Filella (2010), Patterns and controls of the variability of radiation use efficiency and primary productivity across terrestrial ecosystems, *Global Ecol. Biogeogr.*, *19*(2), 253–267, doi:10.1111/j.1466-8238.2009.00504.x.

Gianelle, D., L. Vescovo, B. Marcolla, G. Manca, and A. Cescatti (2009), Ecosystem carbon fluxes and canopy spectral reflectance of a mountain meadow, *Int. J. Remote Sens.*, *30*(2), 435–449, doi:10.1080/01431160802314855.

Giasson, M. A., C. Coursolle, and H. A. Margolis (2006), Ecosystem-level CO_2 fluxes from a boreal cutover in eastern Canada before and after scarification, *Agric. For. Meteorol.*, *140*(1–4), 23–40, doi:10.1016/j.agrformet.2006.08.001.

Gilmanov, T. G., et al. (2007), Partitioning European grassland net ecosystem CO_2 exchange into gross primary productivity and ecosystem respiration using light response function analysis, *Agric. Ecosyst. Environ.*, *121*(1–2), 93–120, doi:10.1016/j.agee.2006.12.008.

Gilmanov, T. G., L. Aires, Z. Barcza, V. S. Baron, L. Belelli, J. Beringer, D. Billesbach, D. Bonal, J. Bradford, and E. Ceschia (2010), Productivity, respiration, and light-response parameters of world grassland and agro ecosystems derived from flux-tower measurements, *Rangeland Ecol. Manage.*, *63*(1), 16–39, doi:10.2111/REM-D-09-00072.1.

Gitelson, A. A., A. Viña, S. B. Verma, D. C. Rundquist, T. J. Arkebauer, G. Keydan, B. Leavitt, V. Ciganda, G. G. Burba, and A. E. Suyker (2006), Relationship between gross primary production and chlorophyll content in crops: Implications for the synoptic monitoring of vegetation productivity, *J. Geophys. Res.*, *111*, D08S11, doi:10.1029/2005JD006017.

Glenn, E. P., P. L. Nagler, and A. Huete (2010), Vegetation index methods for estimating evapotranspiration by remote sensing, *Surv. Geophys.*, *31*(6), 531–555, doi:10.1007/s10712-010-9102-2.

Goldstein, A. H., N. E. Hultman, J. M. Fracheboud, M. R. Bauer, J. A. Panek, M. Xu, Y. Qi, A. B. Guenther, and W. Baugh (2000), Effects of climate variability on the carbon dioxide, water, and sensible heat fluxes above a ponderosa pine plantation in the Sierra Nevada (CA), *Agric. For. Meteorol.*, *101*(2–3), 113–129, doi:10.1016/S0168-1923(99)00168-9.

Gough, C. M., B. S. Hardiman, L. E. Nave, G. Bohrer, K. D. Maurer, C. S. Vogel, K. J. Nadelhoffer, and P. S. Curtis (2013), Sustained carbon uptake and storage following moderate disturbance in a Great Lakes forest, *Ecol. Appl.*, *23*(5), 1202–1215, doi:10.1890/12-1554.1.

Goulden, M. L., B. C. Daube, S. M. Fan, D. J. Sutton, A. Bazzaz, J. W. Munger, and S. C. Wofsy (1997), Physiological responses of a black spruce forest to weather, *J. Geophys. Res.*, *102*(D24), 28,987–28,996, doi:10.1029/97JD01111.

Goulden, M. L., G. C. Winston, A. M. S. McMillan, M. E. Litvak, E. L. Read, A. V. Rocha, and J. R. Elliot (2006), An eddy covariance mesonet to measure the effect of forest age on land-atmosphere exchange, *Global Change Biol.*, *12*(11), 2146–2162, doi:10.1111/j.1365-2486.2006.01251.x.

Groenendijk, M., et al. (2011), Assessing parameter variability in a photosynthesis model within and between plant functional types using global Fluxnet eddy covariance data, *Agric. For. Meteorol.*, *151*, 22–38, doi:10.1016/j.agrformet.2010.08.013.

Grünwald, T., and C. Berhofer (2007), A decade of carbon, water and energy flux measurements of an old spruce forest at the Anchor Station Tharandt, *Tellus, Ser. B*, *59*(3), 387–396, doi:10.1111/j.1600-0889.2007.00259.x.

Gu, L. H., D. Baldocchi, S. B. Verma, T. A. Black, T. Vesala, E. M. Falge, and P. R. Dowty (2002), Advantages of diffuse radiation for terrestrial ecosystem productivity, *J. Geophys. Res.*, *107*(D6), 4050, doi:10.1029/2001JD001242.

Gu, L. H., D. D. Baldocchi, S. C. Wofsy, J. W. Munger, J. J. Michalsky, S. P. Urbanski, and T. A. Boden (2003), Response of a deciduous forest to the Mount Pinatubo eruption: Enhanced photosynthesis, *Science*, *299*, 2035–2038, doi:10.1126/science.1078366.

Gu, L., T. Meyers, S. G. Pallardy, P. J. Hanson, B. Yang, M. Heuer, K. P. Hosman, J. S. Riggs, D. Sluss, and S. D. Wullschleger (2006), Direct and indirect effects of atmospheric conditions and soil moisture on surface energy partitioning revealed by a prolonged drought at a temperate forest site, *J. Geophys. Res.*, *111*, D16102, doi:10.1029/2006JD007161.

Hammer, G. L., and G. C. Wright (1994), A theoretical analysis of nitrogen and radiation effects on radiation use efficiency in peanut, *Aust. J. Agric. Res.*, *45*(3), 575–589, doi:10.1071/AR9940575.

Harada, T., et al. (2010), Application of Akaike information criterion to evaluate warfarin dosing algorithm, *Thromb. Res.*, *126*(3), 183–190, doi:10.1016/j.thromres.2010.05.016.

He, M. Z., et al. (2013), Development of a two-leaf light use efficiency model for improving the calculation of terrestrial gross primary productivity, *Agric. For. Meteorol.*, *173*, 28–39, doi:10.1016/j.agrformet.2013.01.003.

Heinsch, F. A., et al. (2006), Evaluation of remote sensing based terrestrial productivity from MODIS using regional tower eddy flux network observations, *IEEE Trans. Geosci. Remote Sens.*, *44*(7), 1908–1925, doi:10.1109/TGRS.2005.853936.

Hilton, T. W., K. J. Davis, and K. Keller (2014), Evaluating terrestrial CO_2 flux diagnoses and uncertainties from a simple land surface model and its residuals, *Biogeosciences*, *11*(2), 217–235, doi:10.5194/bg-11-217-2014.

Hirata, R., et al. (2008), Spatial distribution of carbon balance in forest ecosystems across East Asia, *Agric. For. Meteorol.*, *148*(5), 761–775, doi:10.1016/j.agrformet.2007.11.016.

Hollinger, D. Y., F. M. Kelliher, J. N. Byers, J. E. Hunt, T. M. McSeveny, and P. L. Weir (1994), Carbon dioxide exchange between an undisturbed old-growth temperate forest and the atmosphere, *Ecology*, *75*(1), 134–150, doi:10.2307/1939390.

Horn, J. E., and K. Schulz (2011), Identification of a general light use efficiency model for gross primary production, *Biogeosciences*, *8*(4), 999–1021, doi:10.5194/bg-8-999-2011.

Humphreys, E. R., T. A. Black, K. Morgenstern, T. Cai, G. B. Drewitt, Z. Nesic, and J. A. Trofymow (2006), Carbon dioxide fluxes in coastal Douglas-fir stands at different stages of development after clearcut harvesting, *Agric. For. Meteorol.*, *140*(1–4), 6–22, doi:10.1016/j.agrformet.2006.03.018.

Ibrom, A., P. G. Jarvis, R. B. Clement, K. Morgenstern, A. Oltchev, B. Medlyn, Y. P. Wang, L. Wingate, J. Moncrieff, and G. Gravenhorst (2006), A comparative analysis of simulated and observed photosynthetic CO_2 uptake in two coniferous forest canopies, *Tree Physiol.*, *26*(7), 845–864, doi:10.1093/treephys/26.7.845.

Ibrom, A., A. Oltchev, T. June, H. Kreilein, G. Rakkibu, T. Ross, O. Panferov, and G. Gravenhorst (2008), Variation in photosynthetic light-use efficiency in a mountainous tropical rain forest in Indonesia, *Tree Physiol.*, *28*(4), 499–508, doi:10.1093/treephys/28.4.499.

Inouye, T., S. Toi, and Y. Matsumoto (1995), A new segmentation method of electroencephalograms by use of Akaike's information criterion, *Cognit. Brain Res.*, *3*(1), 33–40, doi:10.1016/0926-6410(95)00016-X.

Jarvis, P., and S. Linder (2000), Botany: Constraints to growth of boreal forests, *Nature*, *405*, 904–905, doi:10.1038/35016154.

Jenkins, J. P., A. D. Richardson, B. H. Braswell, S. V. Ollinger, D. Y. Hollinger, and M. -L. Smith (2007), Refining light-use efficiency calculations for a deciduous forest canopy using simultaneous tower-based carbon flux and radiometric measurements, *Agric. For. Meteorol.*, *143*(1–2), 64–79, doi:10.1016/j.agrformet.2006.11.008.

Jia, B. H., Z. H. Xie, A. G. Dai, C. X. Shi, and F. Chen (2013), Evaluation of satellite and reanalysis products of downward surface solar radiation over East Asia: Spatial and seasonal variations, *J. Geophys. Res. Atmos.*, *118*, 3431–3446, doi:10.1002/jgrd.50353.

Jun, C., Y. Ban, and S. Li (2014), China: Open access to Earth land-cover map, *Nature*, *514*(7523), 434–434.

Kathilankal, J. C., T. L. O. Halloran, A. Schmidt, C. V. Hanson, and B. E. Law (2014), Development of a semi-parametric PAR (Photosynthetically Active Radiation) partitioning model for the United States, version 1.0, *Geosci. Model Dev.*, *7*, 2477–2484, doi:10.5194/gmd-7-2477-2014.

King, D. A., D. P. Turner, and W. D. Ritts (2011), Parameterization of a diagnostic carbon cycle model for continental scale application, *Remote Sens. Environ.*, *115*(7), 1653–1664, doi:10.1016/j.rse.2011.02.024.

Knohl, A., and D. D. Baldocchi (2008), Effects of diffuse radiation on canopy gas exchange processes in a forest ecosystem, *J. Geophys. Res.*, *113*, G02023, doi:10.1029/2007JG000663.

Knohl, A., E. D. Schulze, O. Kolle, and N. Buchmann (2003), Large carbon uptake by an unmanaged 250-year-old deciduous forest in Central Germany, *Agric. For. Meteorol.*, *118*(3–4), 151–167, doi:10.1016/S0168-1923(03)00115-1.

Krishnan, P., T. A. Black, A. G. Barr, N. J. Grant, D. Gaumont-Guay, and Z. Nesic (2008), Factors controlling the interannual variability in the carbon balance of a southern boreal black spruce forest, *J. Geophys. Res.*, *113*, D09109, doi:10.1029/2007JD008965.

Kume, A., K. N. Nasahara, S. Nagai, and H. Muraoka (2011), The ratio of transmitted near-infrared radiation to photosynthetically active radiation (PAR) increases in proportion to the adsorbed PAR in the canopy, *J. Plant Res.*, *124*(1), 99–106, doi:10.1007/s10265-010-0346-1.

Kutsch, W. L., et al. (2010), The net biome production of full crop rotations in Europe, Agriculture, *Ecosyst. Environ.*, *139*(3), 336–345, doi:10.1016/j.agee.2010.07.016.

Lagergren, F., A. Lindroth, E. Dellwik, A. Ibrom, H. Lankreijer, S. Launiainen, M. Mölder, P. Kolari, K. Pilegaard, and T. Vesala (2008), Biophysical controls on CO_2 fluxes of three Northern forests based on long-term eddy covariance data, *Tellus, Ser. B*, *60*(2), 143–152, doi:10.1111/j.1600-0889.2006.00324.x.

Lamaud, E., Y. Brunet, and P. Berbigier (1997), Radiation and water use efficiencies of two coniferous forest canopies, *Phys. Chem. Earth*, *21*(5), 361–365, doi:10.1016/S0079-1946(97)81124-X.

Lasslop, G., M. Reichstein, D. Papale, A. D. Richardson, A. Arneth, A. Barr, P. Stoy, and G. Wohlfahrt (2010), Separation of net ecosystem exchange into assimilation and respiration using a light response curve approach: Critical issues and global evaluation, *Global Change Biol.*, *16*(1), 187–208, doi:10.1111/j.1365-2486.2009.02041.x.

Law, B. E., et al. (2002), Environmental controls over carbon dioxide and water vapor exchange of terrestrial vegetation, *Agric. For. Meteorol.*, *113*(1–4), 97–120, doi:10.1016/S0168-1923(02)00104-1.

Leuning, R., H. A. Cleugh, S. J. Zegelin, and D. Hughes (2005), Carbon and water fluxes over a temperate Eucalyptus forest and a tropical wet/dry savanna in Australia: Measurements and comparison with MODIS remote sensing estimates, *Agric. For. Meteorol.*, *129*(3–4), 151–173, doi:10.1016/j.agrformet.2004.12.004.

Liu, J., J. M. Chen, J. Cihlar, and W. M. Park (1997), A process-based boreal ecosystem productivity simulator using remote sensing inputs, *Remote Sens. Environ.*, *62*(2), 158–175, doi:10.1016/S0034-4257(97)00089.

Lloyd, J., and J. Taylor (1994), On the temperature dependence of soil respiration, *Funct. Ecol.*, *8*, 315–323, doi:10.2307/2389824.

Lloyd, J., O. Shibistova, D. Zolotoukhine, O. Kolle, A. Arneth, C. Wirth, J. M. Styles, N. M. Tchebakova, and E.-D. Schulze (2002), Seasonal and annual variations in the photosynthetic productivity and carbon balance of a central Siberian pine forest, *Tellus, Ser. B*, *54*(5), 590–610, doi:10.1034/j.1600-0889.2002.01487.x.

Lucht, W., C. B. Schaaf, and A. H. Strahler (2000), An algorithm for the retrieval of albedo from space using semiempirical BRDF models, *Geosci. Remote Sens.*, *38*(2), 977–998, doi:10.1109/36.841980.

Manakos, I., K. Chatzopoulos-Vouzoglanis, Z. I. Petrou, L. Filchev, and A. Apostolakis (2014), Globalland30 mapping capacity of land surface water in Thessaly, Greece, *Land*, *4*(1), 1–18.

Marcolla, B., A. Pitacco, and A. Cescatti (2003), Canopy architecture and turbulence structure in a coniferous forest, *Boundary Layer Meteorol.*, *108*(1), 39–59, doi:10.1023/A:1023027709805.

McCaughey, J. H., M. R. Pejam, M. A. Arain, and D. A. Cameron (2006), Carbon dioxide and energy fluxes from a boreal mixedwood forest ecosystem in Ontario, Canada, *Agric. For. Meteorol.*, *140*(1–4), 79–96, doi:10.1016/j.agrformet.2006.08.010.

Mercado, L. M., N. Bellouin, S. Sitch, O. Boucher, C. Huntingford, M. Wild, and P. M. Cox (2009), Impact of changes in diffuse radiation on the global land carbon sink, *Nature*, *458*, 1014–1017, doi:10.1038/nature07949.

Milyukova, I. M., O. Kolle, A. V. Varlagin, N. N. Vygodskaya, E.-D. Schulze, and J. Lloyd (2002), Carbon balance of a southern taiga spruce stand in European Russia, *Tellus, Ser. B*, *54*(5), 429–442, doi:10.1034/j.1600-0889.2002.01387.x.

Monson, R. K., A. A. Turnipseed, J. P. Sparks, P. C. Harley, L. E. Scott-Denton, K. Sparks, and T. E. Huxman (2002), Carbon sequestration in a high-elevation, subalpine forest, *Global Change Biol.*, *8*(5), 459–478, doi:10.1046/j.1365-2486.2002.00480.x.

Montagnani, L., et al. (2009), A new mass conservation approach to the study of CO_2 advection in an alpine forest, *J. Geophys. Res.*, *114*, D07306, doi:10.1029/2008JD010650.

Monteith, J. L. (1972), Solar radiation and productivity in tropical ecosystems, *J. Appl. Ecol.*, *9*(3), 747–766, doi:10.2307/2401901.

Niyogi, D., et al. (2004), Direct observations of the effects of aerosol loading on net ecosystem CO_2 exchanges over different landscapes, *Geophys. Res. Lett.*, *31*, L20506, doi:10.1029/2004GL020915.

Noormets, A., M. J. Gavazzi, S. G. McNulty, J. C. Domec, G. Sun, J. S. King, and J. Chen (2010), Response of carbon fluxes to drought in a coastal plain loblolly pine forest, *Global Change Biol.*, *16*(1), 272–287, doi:10.1111/j.1365-2486.2009.01928.x.

Papale, D., and R. Valentini (2003), A new assessment of European forests carbon exchanges by eddy fluxes and artificial neural network spatialization, *Global Change Biol.*, *9*(4), 525–535, doi:10.1046/j.1365-2486.2003.00609.x.

Papale, D., et al. (2006), Towards a standardized processing of net ecosystem exchange measured with eddy covariance technique: Algorithms and uncertainty estimation, *Biogeosciences*, *3*(4), 571–583, doi:10.5194/bg-3-571-2006.

Pataki, D. E., and R. Oren (2003), Species differences in stomatal control of water loss at the canopy scale in a mature bottomland deciduous forest, *Adv. Water Resour.*, *26*(12), 1267–1278, doi:10.1016/j.advwatres.2003.08.001.

Potter, C. S., J. T. Randerson, C. B. Field, P. A. Matson, P. M. Vitousek, H. A. Mooney, and S. A. Klooster (1993), Terrestrial ecosystem production: A process model based on global satellite and surface data, *Global Biogeochem. Cycles*, *7*(4), 811–841, doi:10.1029/93GB02725.

Powell, T. L., R. Bracho, J. Li, S. Dore, C. R. Hinkle, and B. G. Drake (2006), Environmental controls over net ecosystem carbon exchange of scrub oak in central Florida, *Agric. For. Meteorol.*, *141*(1), 19–34, doi:10.1016/j.agrformet.2006.09.002.

Price, D. T., and T. A. Black (1990), Effects of short-term variation in weather on diurnal canopy CO_2 flux and evapotranspiration of a juvenile Douglas fir stand, *Agric. For. Meteorol.*, *50*(3), 139–158, doi:10.1016/0168-1923(90)90050-G.

Prince, S. D., and S. N. Goward (1995), Global primary production: A remote sensing Asproach, *J. Biogeogr.*, *22*(4–5), 815–835, doi:10.2307/2845983.

Propastin, P., A. Ibrom, A. Knohl, and S. Erasmi (2012), Effects of canopy photosynthesis saturation on the estimation of gross primary productivity from MODIS data in a tropical forest, *Remote Sens. Environ.*, *121*, 252–260, doi:10.1016/j.rse.2012.02.005.

Rebmann, C., M. Zeri, G. Lasslop, M. Mund, O. Kolle, E. D. Schulze, and C. Feigenwinter (2010), Treatment and assessment of the CO_2-exchange at a complex forest site in Thuringia, Germany, *Agric. For. Meteorol.*, *150*(5), 684–691, doi:10.1016/j.agrformet.2009.11.001.

Reichstein, M., et al. (2005), On the separation of net ecosystem exchange into assimilation and ecosystem respiration: Review and improved algorithm, *Global Change Biol.*, *11*(9), 1424–1439, doi:10.1111/j.1365-2486.2005.001002.x.

Rochette, P., R. L. Desjardins, E. Pattey, and R. Lessard (1996), Instantaneous measurement of radiation and water use efficiencies of a maize crop, *Agron. J.*, *88*(4), 627–635, doi:10.2134/agronj1996.00021962008800040022x.

Roderick, M., G. Farquhar, S. Berry, and I. Noble (2001), On the direct effect of clouds and atmospheric particles on the productivity and structure of vegetation, *Oecologia*, *129*(1), 21–30, doi:10.1007/s004420100760.

Román, M. O., et al. (2009), The MODIS (Collection V005) BRDF/albedo product: Assessment of spatial representativeness over forested landscapes, *Remote Sens. Environ.*, *113*(11), 2476–2498, doi:10.1016/j.rse.2009.07.009.

Roupsard, O., et al. (2006), Partitioning energy and evapo-transpiration above and below a tropical palm canopy, *Agric. For. Meteorol.*, *139*(3–4), 252–268, doi:10.1016/j.agrformet.2006.07.006.

Running, S. W., D. D. Baldocchi, D. P. Turner, S. T. Gower, P. S. Bakwin, and K. A. Hibbard (1999), A global terrestrial monitoring network integrating tower fluxes, flask sampling, ecosystem modeling and EOS satellite data, *Remote Sens. Environ.*, *70*(1), 108–127, doi:10.1016/S0034-4257(99)00061-9.

Running, S. W., P. E. Thornton, R. Nemani, and J. M. Glassy (2000), Global terrestrial gross and net primary productivity from the Earth Observing System, in *Methods in Ecosystem Science*, pp. 44–55, Springer, New York, doi:10.1007/978-1-4612-1224-9-4.

Running, S. W., R. R. Nemani, F. A. Heinsch, M. S. Zhao, M. Reeves, and H. Hashimoto (2004), A continuous satellite-derived measure of global terrestrial primary production, *BioScience*, *54*(6), 547–560, doi:10.1641/0006-3568(2004)054[0547:ACSMOG]2.0.CO;2.

Russell, G., P. G. Jarvis, and J. L. Monteith (1989), Absorption of radiationby canopies and stand growth, in *Plant Canopies: Their Growth, Form and Function*, edited by G. Russell, B. Marshall, and P. G. Jarvis, pp. 21–39, Cambridge Univ. Press, Cambridge, U. K.

Ryu, Y., et al. (2011), Integration of MODIS land and atmosphere products with a coupled-process model to estimate gross primary productivity and evapotranspiration from 1 km to global scales, *Global Biogeochem. Cycles*, *25*, GB4017, doi:10.1029/2011GB004053.

Sakamoto, T., A. A. Gitelson, B. D. Wardlow, S. B. Verma, and A. E. Suyker (2011), Estimating daily gross primary production of maize based only on MODIS WDRVI and shortwave radiation data, *Remote Sens. Environ.*, *115*(12), 3091–3101, doi:10.1016/j.rse.2011.06.015.

Schaaf, C. B., et al. (2002), First operational BRDF, albedo nadir reflectance products from MODIS, *Remote Sens. Environ.*, *83*(1–2), 135–148, doi:10.1016/S0034-4257(02)00091-3.

Schmid, H. P. (1997), Experimental design for flux measurements: Matching scales of observations and fluxes, *Agric. For. Meteorol.*, *87*(2–3), 179–200, doi:10.1016/S0168-1923(97)00011-7.

Schmid, H. P. (2002), Footprint modeling for vegetation atmosphere exchange studies: A review and perspective, *Agric. For. Meteorol.*, *113*(1–4), 159–183, doi:10.1016/S0168-1923(02)00107-7.

Schmid, H. P., C. S. B. Grimmond, F. Cropley, B. Offerle, and H. B. Su (2000), Measurements of CO_2 and energy fluxes over a mixed hardwood forest in the mid-western United States, *Agric. For. Meteorol.*, *103*(4), 357–374, doi:10.1016/S0168-1923(00)00140-4.

Scott, R. L. (2010), Using watershed water balance to evaluate the accuracy of eddy covariance evaporation measurements for three semiarid ecosystems, *Agric. For. Meteorol.*, *150*(2), 219–225, doi:10.1016/j.agrformet.2009.11.002.

Sinclair, T. R., and T. Shiraiwa (1993), Soybean radiation-use efficiency as influenced by nonuniform specific leaf nitrogen distribution and diffuse radiation, *Crop Sci.*, *33*(4), 808–812, doi:10.2135/cropsci1993.0011183X003300040036x.

Sinclair, T. R., T. Shiraiwa, and G. L. Hammer (1992), Variation in crop radiation use efficiency with increased diffuse radiation, *Crop Sci.*, *32*(5), 1281–1284, doi:10.2135/cropsci1992.0011183X003200050043x.

Sjöström, M., et al. (2013), Evaluation of MODIS gross primary productivity for Africa using eddy covariance data, *Remote Sens. Environ.*, *131*, 275–286, doi:10.1016/j.rse.2012.12.023.

Smith, P., G. Lanigan, W. L. Kutsch, N. Buchmann, W. Eugster, M. Aubinet, E. Ceschia, P. Béziat, J. B. Yeluripati, and B. Osborne (2010), Measurements necessary for assessing the net ecosystem carbon budget of croplands, *Agric. Ecosyst. Environ.*, *139*(3), 302–315, doi:10.1016/j.agee.2010.04.004.

Sprintsin, M., S. Cohen, K. Maseyk, E. Rotenberg, J. Grünzweig, A. Karnieli, P. Berliner, and D. Yakir (2011), Long term and seasonal courses of leaf area index in a semi-arid forest plantation, *Agric. For. Meteorol.*, *151*(5), 565–574, doi:10.1016/j.agrformet.2011.01.001.

Stanhill, G., and S. Cohen (2001), Global dimming: A review of the evidence for a widespread and significant reduction in global radiation with discussion of its probable causes and possible agricultural consequences, *Agric. For. Meteorol.*, *107*(4), 255–278, doi:10.1016/S0168-1923(00)00241-0.

Stoy, P. C., et al. (2013), A data-driven analysis of energy balance closure across FLUXNET research sites: The role of landscape scale heterogeneity, *Agric. For. Meteorol.*, *171–172*, 137–152, doi:10.1016/j.agrformet.2012.11.004.

Suni, T., J. Rinne, A. Reissell, N. Altimir, P. Keronen, Ü. Rannik, M. D. Maso, M. Kulmala, and T. Vesala (2003), Long-term measurements of surface fluxes above a Scots pine forest in Hyytiälä, southern Finland, 1996–2001, *Boreal Environ. Res.*, *8*(4), 287–301.

Tang, S., J. M. Chen, Q. Zhu, X. Li, M. Chen, R. Sun, Y. Zhou, F. Deng, and D. Xie (2007), LAI inversion algorithm based on directional reflectance kernels, *J. Environ. Manage.*, *85*, 638–648, doi:10.1016/j.jenvman.2006.08.01.

Tsubo, M., and S. Walker (2005), Relationships between photosynthetically active radiationand clearness index at Bloemfontein, South Africa, *Theor. Appl. Climatol.*, *80*(1), 17–25, doi:10.1007/s00704-004-0080-5.
Turner, D. P., et al. (2006), Evaluation of MODIS NPP and GPP products across multiple biomes, *Remote Sens. Environ.*, *102*(3–4), 282–292, doi:10.1016/j.rse.2006.02.017.
Urban, O., et al. (2007), Ecophysiological controls over the net ecosystem exchange of mountain spruce stand. Comparison of the response in direct vs. diffuse solar radiation, *Global Change Biol.*, *13*(1), 157–168, doi:10.1111/j.1365-2486.2006.01265.x.
Veroustraete, F., H. Sabbe, and H. Eerens (2002), Estimation of carbon mass fluxes over Europe using the C-Fix model and Euroflux data, *Remote Sens. Environ.*, *83*, 376–399, doi:10.1016/S0034-4257(02)00043-3.
Vickers, D., C. Thomas, and B. E. Law (2009), Random and systematic CO_2 flux sampling errors for tower measurements over forests in the convective boundary layer, *Agric. For. Meteorol.*, *149*(1), 73–83, doi:10.1016/j.agrformet.2008.07.005.
Wang, Y., and Q. Liu (2006), Comparison of Akaike information criterion (AIC) and Bayesian information criterion (BIC) in selection of stock-recruitment relationships, *Fish. Res.*, *77*, 220–225, doi:10.1016/j.fishres.2005.08.011.
Wang, Y. P., and R. Leuning (1998), A two-leaf model for canopy conductance, photosynthesis and partitioning of available energy I: Model description and comparison with a multi-layered model, *Agric. For. Meteorol.*, *91*(1–2), 89–111, doi:10.1016/S0168-1923(98)00061-6.
Wang, Y. P., R. Leuning, H. A. Cleug, and P. A. Coppin (2001), Parameter estimation in surface exchange models using nonlinear inversion: How many parameters can we estimate and which measurements are most useful?, *Global Change Biol.*, *7*(5), 495–510, doi:10.1046/j.1365-2486.2001.00434.x.
Wei, S., et al. (2014), Data-based perfect-deficit approach to understanding climate extremes and forest carbon assimilation capacity, *Environ. Res. Lett.*, *9*(6), 065002, doi:10.1088/1748-9326/9/6/065002.
Weiss, A., and J. M. Norman (1985), Partitioning solar radiation into direct and diffuse, visible and near-infrared components, *Agric. For. Meteorol.*, *34*(2–3), 205–213, doi:10.1016/0168-1923(85)90020-6.
Willmott, C. J. (1981), On the validation of models, *Phys. Geogr.*, *2*, 184–194, doi:10.1080/02723646.1981.10642213.
Willmott, C. T. (1982), Some comments on the evaluation of model performance, *Bull. Am. Meteorol. Soc.*, *63*(11), 1310–1313, doi:10.1175/1520-0477(1982)063<1309:SCOTEO>2.0.CO;2.
Wohlfahrt, G., A. Hammerle, A. Haslwanter, M. Bahn, U. Tappeiner, and A. Cernusca (2008), Disentangling leaf area and environmental effects on the response of the net ecosystem CO2 exchange to diffuse radiation, *Geophys. Res. Lett.*, *35*, L16805, doi:10.1029/2008GL035090.
Wu, C. Y., J. Chen, and Z. Niu (2011), Predicting gross primary production from the enhanced vegetation index and photosynthetically active radiation: Evaluation and calibration, *Remote Sens. Environ.*, *115*(12), 3424–3435, doi:10.1016/j.rse.2011.08.006.
Xiao, J., et al. (2008), Estimation of net ecosystem carbon exchange for the conterminous United States by combining MODIS and AmeriFlux data, *Agric. For. Meteorol.*, *148*, 1827–1847, doi:10.1016/j.agrformet.2008.06.015.
Xiao, J. F., et al. (2011), Assessing net ecosystem carbon exchange of U. S. terrestrial ecosystems by integrating eddy covariance flux measurements and satellite observations, *Agric. For. Meteorol.*, *151*(1), 60–69, doi:10.1016/j.agrformet.2010.09.002.
Xiao, X. M., Q. Y. Zhang, B. Braswell, S. Urbanski, S. Boles, S. Wofsy, B. Moore, and D. Ojima (2004), Modeling gross primary production of temperate deciduous broadleaf forest using satellite images and climate data, *Remote Sens. Environ.*, *91*(2), 256–270, doi:10.1016/j.rse.2004.03.010.
Xu, L. K., and D. D. Baldocchi (2004), Seasonal variation in carbon dioxide exchange over a Mediterranean annual grassland in California, *Agric. For. Meteorol.*, *123*(1–2), 79–96, doi:10.1016/j.agrformet.2003.10.004.
Yu, G. R., X. F. Wen, X. M. Sun, B. D. Tanner, X. H. Lee, and J. Y. Chan (2006), Overview of ChinaFLUX and evaluation of its eddy covariance measurement, *Agric. For. Meteorol.*, *137*(3–4), 125–137, doi:10.1016/j.agrformet.2006.02.011.
Yuan, W. P., et al. (2007), Deriving a light use efficiency model from eddy covariance flux data for predicting daily gross primary production across biomes, *Agric. For. Meteorol.*, *143*(3–4), 189–207, doi:10.1016/j.agrformet.2006.12.001.
Yuan, W. P., et al. (2010), Global estimates of evapotranspiration and gross primary production based on MODIS and global meteorology data, *Remote Sens. Environ.*, *114*(7), 1416–1431, doi:10.1016/j.rse.2010.01.022.
Zha, T. S., et al. (2009), Carbon sequestration in boreal jack pine stands following harvesting, *Global Change Biol.*, *15*(6), 1475–1487, doi:10.1111/j.1365-2486.2008.01817.x.
Zhang, M., et al. (2011), Effects of cloudiness change on net ecosystem exchange, light use efficiency and water use efficiency in typical ecosystems of China, *Agric. For. Meteorol.*, *151*(7), 803–816, doi:10.1016/j.agrformet.2011.01.011.
Zhang, Y. J., M. Xu, H. Chen, and J. Adams (2009), Global pattern of NPP to GPP ratio derived from MODIS data: Effects of ecosystem type, geographical location and climate, *Global Ecol. Biogeogr.*, *18*(3), 280–290, doi:10.1111/j.1466-8238.2008.00442.x.
Zhang, Y. Q., Q. Yu, J. Jiang, and Y. H. Tang (2008), Calibration of Terra/MODIS gross primary production over an irrigated cropland on the North China Plain and an alpine meadow on the Tibetan Plateau, *Global Change Biol.*, *14*(4), 757–767, doi:10.1111/j.1365-2486.2008.01538.x.
Zhao, M. S., and S. W. Running (2006), Sensitivity of Moderate Resolution Imaging Spectroradiometer (MODIS) terrestrial primary production to the accuracy of meteorological reanalyses, *J. Geophys. Res.*, *111*, G01002, doi:10.1029/2004JG000004.
Zhao, M. S., F. A. Heinsch, R. R. Nemani, and S. W. Running (2005), Improvements of the MODIS terrestrial gross and net primary production global data set, *Remote Sens. Environ.*, *95*(2), 164–176, doi:10.1016/j.rse.2004.12.011.